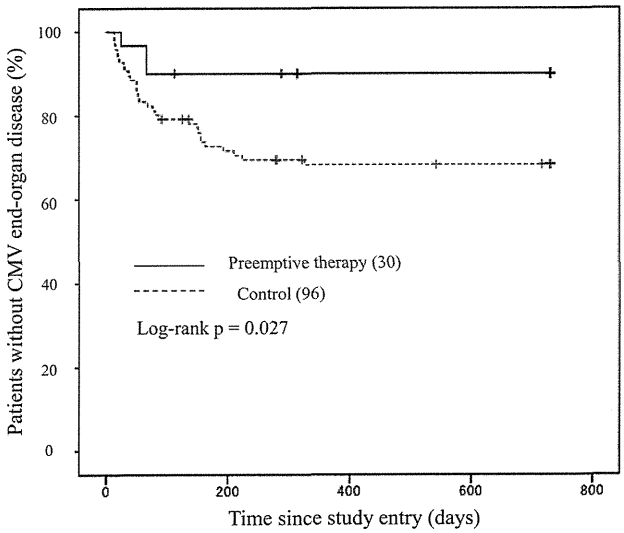

Figure 2. Kaplan-Meier curve showing the time to development of cytomegalovirus (CMV)- end-organ disease (EOD) in the preemptive and non-preemptive therapy groups. Compared to patients on CMV preemptive therapy, those who did not receive preemptive therapy were more likely to develop CMV-EOD (p = 0.027, Log-rank test).
doi:10.1371/journal.pone.0065348.g002

count, use of steroids, chemotherapy, and concurrent AIDS defining diseases were not associated with CMV-EOD. Multivariate analysis identified CMV preemptive therapy as a significant preventive factor against CMV-EOD after adjustment for age and sex (Model 2; adjusted HR = 0.289; 95%CI, 0.088–0.949; p = 0.041, Table 3), and after adjustment for other risk factors (Model 3; adjusted HR = 0.172; 95%CI, 0.049–0.602; p = 0.005, Table 3). In addition, multivariate analysis showed that high CMV viral load correlated significantly with CMV-EOD (Model 3; adjusted HR = 1.941; 95%CI, 1.266–2.975; p = 0.002, Table 3).

Of the 33 patients with CMV-EOD, 22 (66.7%) developed CMV retinitis, 4 (12.1%) developed esophagitis, 3 (9.1%) developed gastroduodenitis, 6 (18.2%) developed colitis and 1 (3.0%) developed pneumonitis. All 3 patients with CMV-EOD of the preemptive therapy group developed retinitis (Table 4).

Table 2. Results of univariate analysis to estimate the risk of various factors in inducing CMV end-organ disease.

	Hazard ratio	95% CI	P value
CMV preemptive therapy	0.286	0.087–0.939	0.039
Female	1.284	0.392–4.209	0.680
Age per 1 year	0.982	0.951–1.013	0.240
CD4 count per 1/μl decrement	1.001	0.989–1.013	0.867
HIV viral load per log10/ml	1.875	0.905–3.884	0.091
CMV viral load per log10/ml	1.450	0.984–2.136	0.060
Use of steroid	0.716	0.356–1.439	0.348
Chemotherapy	1.390	0.488–3.955	0.537
Concurrent AIDS	0.703	0.290–1.704	0.436

CI: confidence interval
The Cox proportional hazards regression analysis was used.
doi:10.1371/journal.pone.0065348.t002

Of 30 patients who received preemptive therapy, 20 (66.7%) received an induction dose of GCV, and 7 patients (23.3%) received maintenance dose. The remaining agents used for preemptive therapy were an induction dose of VGCV, a maintenance dose of FOS and an induction dose of cidofovir. The duration of the preemptive therapy varied between 7 days and 2 months. The following side effects were noted in patients on CMV preemptive therapy: grade 3/4 leukopenia (n = 7, 23.3%) and grade 2 hypercreatininemia (n = 1, 3.3%). Both side effects developed during the use of GCV. Five patients (5.2%) of the non-preemptive therapy group and 4 patients (13.3%) of the preemptive therapy group died during the study period. Of the former group, 3 deaths were due to opportunistic infections (cryptococcus meningitis, non-tuberculous mycobacterial infection and *Pneumocystis jiroveci* pneumonia), 1 due to bacterial infection (sepsis), and 1 due to suicide. Of the latter group, 2 deaths were due to opportunistic infections (malignant lymphoma and *P. jiroveci* pneumonia) and 2 due to bacterial infection (bacterial pneumonias). Deaths and bacterial infections related to preemptive therapy were not observed in our study. The mortality rate was not significantly different between the two groups (p = 0.193, Log-rank test, Figure 3).

Discussion

The results of this observational cohort of treatment-naïve HIV-infected patients with positive plasma CMV DNA showed a significantly lower incidence of CMV-EOD by one-fourths in the CMV preemptive therapy group than in the non-preemptive therapy group, over the 2-year observation period. This finding was significant, despite higher risk for CMV-EOD in the preemptive therapy group, such as higher plasma CMV DNA, higher prevalence of concurrent AIDS defining diseases and more concurrent steroid use, compared with the other group. Univariate and multivariate analyses identified anti-CMV preemptive therapy as a significant preventive factor against CMV-EOD.

Our study is the first to illustrate the significance of anti-CMV preemptive therapy in treatment- naïve HIV-infected patients with CMV viremia and CD4 count less than 100/μl in the HAART era. The hazard ratio of development of CMV-EOD decreased by 82.8% following preemptive therapy, compared with no preemptive therapy, even after adjustment for plasma CMV DNA viral load and other factors. The current guidelines do not generally recommend anti-CMV preemptive therapy although this is based on sparse evidence, such as cost effectiveness, CMV resistance, and drug side effects [7]. However, our study suggests that preemptive therapy is a feasible option, if the effective target of preemptive therapy could be selected. Furthermore, the study confirmed that plasma CMV DNA, a known risk factor for CMV-EOD [12–18], was a significant independent risk factor.

A few prospective clinical trials investigated the efficacy of preemptive therapy in both the pre-HAART era and HAART era. In these studies, oral GCV at 1000 mg thrice daily was used in the pre-HAART era regimen [9,10] while VGCV at 900 mg twice daily was the regimen used in the HAART era [11]. The patients investigated in the above three studies were HIV-treatment-experienced patients. One study in the pre-HAART era reported the efficacy of preemptive therapy in patients with CD4 count<50 μl [9], while the other studies showed no significant preventive effect [10,11]. In the ACTG A5030 study, the prospective clinical trial in the HAART era, which evaluated the efficacy of oral VGCV 900 mg twice a day for 3 weeks among HIV-infected patients with CD4 count <100 cells/mm^3, plasma HIV RNA >400 copies/mL, plasma CMV viremia and on stable

Table 3. Results of multivariate analysis to estimate the preventive effect of CMV preemptive therapy against CMV end-organ disease.

	Model 1 Crude		Model 2 Adjusted		Model 3 Adjusted	
	HR	95% CI	HR	95%CI	HR	95%CI
CMV preemptive therapy*	0.286	0.087–0.939	0.289	0.088–0.949	0.172	0.049–0.602
Age			0.982	0.952–1.014	0.990	0.958–1.022
Female			1.033	0.310–3.441	0.988	0.267–3.653
CD4 count per 1/μl decrement					0.995	0.983–1.008
HIV viral load per log10/ml					2.217	0.912–5.393
CMV viral load per log10/ml*					1.941	1.266–2.975
Use of steroid					0.664	0.288–1.534
Chemotherapy					1.668	0.540–5.151
Concurrent AIDS					0.930	0.337–2.569

*P<0.05 in Model 3
HR: hazard ratio, CI: confidence interval
The Cox proportional hazards regression analysis was used.
Variables with significant difference by univariate analysis or assumed as risk factors for CMV-EOD in the literature were included in model 3.
doi:10.1371/journal.pone.0065348.t003

or no HAART, the authors reported a low incidence of CMV-EOD among subjects both with and without preemptive therapy [11]. The authors attributed the low incidence to improvement of immune function induced by potent ART. Actually, in that study [11], the number of patients who had received ART at study entry was about 80% of the total. In contrast, the subjects of our study were all treatment-naïve patients and possibly at higher risk for CMV-EOD compared to those enrolled in the ACTG A5030. Thus, the use of CMV preemptive therapy reported in our study under the clinical scenario of poor immune status without ART at study entry resulted in better outcome than in previous studies. In our study, there was no significant difference in the timing of ART between the two treatment groups. Although our study did not include the time to the initiation of ART as a variable in uni- and multivariate analysis because the values for 11 cases were missing, multivariate analysis with the time to the initiation of ART together with other variables similarly identified preemptive therapy as a significant preventive factor (adjusted HR = 0.235; 95%CI, 0.064–0.868; p = 0.030).

The survival benefits of CMV preemptive therapy were controversial in previous prospective clinical trials. One study suggested the survival benefits of 3 g/day oral GCV preemptive therapy [9], while other studies showed no evidence of the survival benefit [10]. On the other hand, two prospective cohort studies in the HAART era showed the relation between CMV viremia and high mortality [21] and suggested the benefit of CMV therapy [22], whereas our results showed no significant difference in mortality rate between the two groups. The reason for this discrepancy could be attributed to low mortality rate, small sample size and the disproportionally high risk of the therapy group in our study. The mortality rate (5.0 deaths per 100 person-years) in our study was similar to that in a study conducted in the HAART era (5.7 deaths per 100 person-years)[19] and was considerably lower than in studies from the pre-HAART era. Since the mortality rate has markedly decreased in advanced HIV infected patients following the introduction of potent ART in the HAART era [23,24], not only the survival benefit but also quality of life, such as improvement of eye function, should be emphasized in the future.

The side effects of preemptive therapy have also been of concern [25]. Our findings showed the development of grade 3 to 4 leukocytopenia in 23.3% of the patients who received intravenous GCV, and was the major side effect of preemptive therapy. Some patients who developed leukocytopenia required treatment with granulocyte colony-stimulating factor (G-CSF) and showed complete recovery. Thus; careful follow-up of patients on preemptive therapy is necessary. For these reasons, preemptive

Table 4. Details of CMV end-organ disease.

CMV-EOD	n (%)	Time to development (days)	Non-preemptive therapy group	Preemptive therapy group
Retinitis	22* (61.1%)	72 (14–326)	19* (57.6%)	3 (100%)
Esophagitis	4* (11.1%)	116.5(69–164)	4* (12.1%)	0
Gastroenteritis	3* (8.3%)	19 (14–40)	3* (9.1%)	0
Colitis	6* (16.7%)	40.5 (15–55)	6* (18.2%)	0
Pneumonitis	1 (2.8%)	31 (31–31)	1 (3.0%)	0
Total	36* (100%)	55 (14–326)	33* (100%)	3 (100%)

*Three patients of the non-preemptive therapy group had multiple CMV-EOD; one with retinitis plus esophagitis, one with retinitis plus gastroenteritis and the other with retinitis plus colitis.
doi:10.1371/journal.pone.0065348.t004

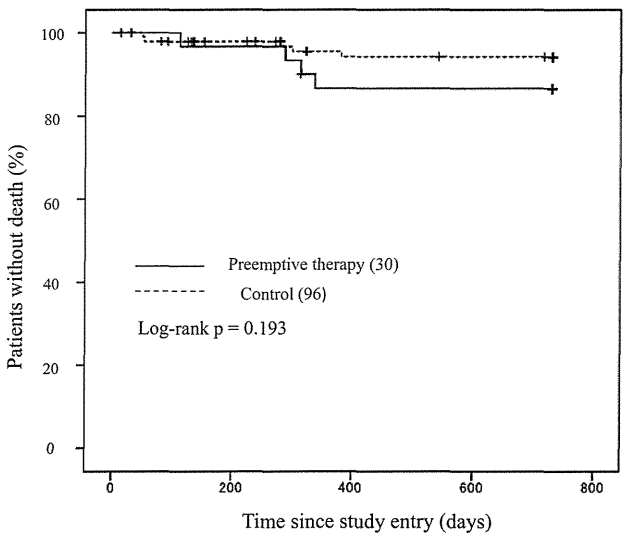

Figure 3. Kaplan-Meier curve showing the time to death in the preemptive and non-preemptive therapy groups. There was no significant difference in the survival rate between the two groups (p = 0.193, Log-rank test).
doi:10.1371/journal.pone.0065348.g003

therapy might place patients at greater risk in resource-limited setting, where close monitoring is difficult and the risk of bacterial infection is high. It is noteworthy, however, that death and bacterial infection related to preemptive therapy were not observed in our study.

The present study has several limitations. Due to its retrospective nature, it was not possible to control the baseline characteristics of the enrolled patients. However, patients with potential risk for CMV-EOD, such as those with high plasma CMV DNA, high concurrent AIDS and high steroid use, were more likely prescribed the preemptive therapy. It is noteworthy that the incidence of CMV-EOD was significantly lower in the preemptive therapy group despite this adverse environment.

Second, the criteria for treatment, choice of drugs and duration of CMV preemptive therapy were not rigidly controlled in the present study. Thus, it was difficult to determine which anti-CMV agent with what dosage is optimal for preemptive therapy. In the present study, about 90% of patients received induction dose or maintenance dose of GCV since the majority of patients of the preemptive therapy group were in-patients. Further prospective study is required to optimize effective preemptive therapy, including oral VGCV.

Third, CMV-EOD, especially enteritis, could have been overlooked at study entry since routine endoscopic screening was not performed, compared with screening for retinitis at the first visit. However, patients with abdominal pain were subjected to stool examination for occult blood, since the definition of CMV enteritis includes abdominal pain, and those with positive tests were subsequently considered for endoscopy. Thus, the possibility of latent CMV enteritis at study entry does not seem to have affected the results of the present study.

In conclusion, the present study demonstrated a lower incidence of CMV-EOD following CMV preemptive therapy by one-fourth, compared with no preemptive therapy, in treatment-naïve patients with CMV viremia. High plasma CMV DNA was identified as an independent risk for CMV-EOD. Further studies are warranted to elucidate the efficacy, safety and cost-effectiveness of anti-CMV preemptive therapy in HIV infected patients at high risk for EOD.

Supporting Information

Table S1 Definitions of CMV end-organ diseases used in this study.
(DOCX)

Acknowledgments

The authors thank all the clinical staff at the AIDS Clinical Center for their help in completion of this study.

Author Contributions

Conceived and designed the experiments: DM K. Tsukada K. Teruya. Performed the experiments: DM TN K. Teruya. Analyzed the data: DM HG YK SO. Contributed reagents/materials/analysis tools: YK K. Tsukada. Wrote the paper: DM TN HG SO.

References

1. Jabs DA, Van Natta ML, Holbrook JT, Kempen JH, Meinert CL, et al. (2007) Longitudinal study of the ocular complications of AIDS: 1. Ocular diagnoses at enrollment. Ophthalmology 114: 780–786.
2. Goodrich JM, Mori M, Gleaves CA, Du Mond C, Cays M, et al. (1991) Early treatment with ganciclovir to prevent cytomegalovirus disease after allogeneic bone marrow transplantation. N Engl J Med 325: 1601–1607.
3. Kalil AC, Levitsky J, Lyden E, Stoner J, Freifeld AG (2005) Meta-analysis: the efficacy of strategies to prevent organ disease by cytomegalovirus in solid organ transplant recipients. Ann Intern Med 143: 870–880.
4. Kalil AC, Freifeld AG, Lyden ER, Stoner JA (2009) Valganciclovir for cytomegalovirus prevention in solid organ transplant patients: an evidence-based reassessment of safety and efficacy. PLoS One 4: e5512.
5. Park JM, Lake KD, Arenas JD, Fontana RJ (2006) Efficacy and safety of low-dose valganciclovir in the prevention of cytomegalovirus disease in adult liver transplant recipients. Liver Transpl 12: 112–116.
6. Humar A, Kumar D, Preiksaitis J, Boivin G, Siegal D, et al. (2005) A trial of valganciclovir prophylaxis for cytomegalovirus prevention in lung transplant recipients. Am J Transplant 5: 1462–1468.
7. Kaplan JE, Benson C, Holmes KH, Brooks JT, Pau A, et al. (2009) Guidelines for prevention and treatment of opportunistic infections in HIV-infected adults and adolescents: recommendations from CDC, the National Institutes of Health, and the HIV Medicine Association of the Infectious Diseases Society of America. MMWR Recomm Rep 58: 1–207; quiz CE201-204.
8. Rose DN, Sacks HS (1997) Cost-effectiveness of cytomegalovirus (CMV) disease prevention in patients with AIDS: oral ganciclovir and CMV polymerase chain reaction testing. AIDS 11: 883–887.
9. Spector SA, McKinley GF, Lalezari JP, Samo T, Andruczk R, et al. (1996) Oral ganciclovir for the prevention of cytomegalovirus disease in persons with AIDS. Roche Cooperative Oral Ganciclovir Study Group. N Engl J Med 334: 1491–1497.
10. Brosgart CL, Louis TA, Hillman DW, Craig CP, Alston B, et al. (1998) A randomized, placebo-controlled trial of the safety and efficacy of oral ganciclovir for prophylaxis of cytomegalovirus disease in HIV-infected individuals. Terry Beirn Community Programs for Clinical Research on AIDS. AIDS 12: 269–277.
11. Wohl DA, Kendall MA, Andersen J, Crumpacker C, Spector SA, et al. (2009) Low rate of CMV end-organ disease in HIV-infected patients despite low CD4+ cell counts and CMV viremia: results of ACTG protocol A5030. HIV Clin Trials 10: 143–152.
12. Spector SA, Wong R, Hsia K, Pilcher M, Stempien MJ (1998) Plasma cytomegalovirus (CMV) DNA load predicts CMV disease and survival in AIDS patients. J Clin Invest 101: 497–502.
13. Spector SA, Hsia K, Crager M, Pilcher M, Cabral S, et al. (1999) Cytomegalovirus (CMV) DNA load is an independent predictor of CMV disease and survival in advanced AIDS. J Virol 73: 7027–7030.
14. Pergam SA, Xie H, Sandhu R, Pollack M, Smith J, et al. (2012) Efficiency and Risk Factors for CMV Transmission in Seronegative Hematopoietic Stem Cell Recipients. Biol Blood Marrow Transplant.
15. Kute VB, Vanikar AV, Shah PR, Gumber MR, Patel HV, et al. (2012) Post-renal transplant cytomegalovirus infection: study of risk factors. Transplant Proc 44: 706–709.
16. Fielding K, Koba A, Grant AD, Charalambous S, Day J, et al. (2011) Cytomegalovirus viremia as a risk factor for mortality prior to antiretroviral therapy among HIV-infected gold miners in South Africa. PLoS One 6: e25571.

17. Micol R, Buchy P, Guerrier G, Duong V, Ferradini L, et al. (2009) Prevalence, risk factors, and impact on outcome of cytomegalovirus replication in serum of Cambodian HIV-infected patients (2004-2007). J Acquir Immune Defic Syndr 51: 486–491.
18. Yoshida A, Hitomi S, Fukui T, Endo H, Morisawa Y, et al. (2001) Diagnosis and monitoring of human cytomegalovirus diseases in patients with human immunodeficiency virus infection by use of a real-time PCR assay. Clin Infect Dis 33: 1756–1761.
19. Erice A, Tierney C, Hirsch M, Caliendo AM, Weinberg A, et al. (2003) Cytomegalovirus (CMV) and human immunodeficiency virus (HIV) burden, CMV end-organ disease, and survival in subjects with advanced HIV infection (AIDS Clinical Trials Group Protocol 360). Clin Infect Dis 37: 567–578.
20. Hodge WG, Boivin JF, Shapiro SH, Shah KC, Dionne MA (2005) Iatrogenic risk factors for cytomegalovirus retinitis. Can J Ophthalmol 40: 701–710.
21. Deayton JR, Prof Sabin CA, Johnson MA, Emery VC, Wilson P, et al. (2004) Importance of cytomegalovirus viraemia in risk of disease progression and death in HIV-infected patients receiving highly active antiretroviral therapy. Lancet 363: 2116–2121.
22. Kempen JH, Martin BK, Wu AW, Barron B, Thorne JE, et al. (2003) The effect of cytomegalovirus retinitis on the quality of life of patients with AIDS in the era of highly active antiretroviral therapy. Ophthalmology 110: 987–995.
23. Ray M, Logan R, Sterne JA, Hernandez-Diaz S, Robins JM, et al. (2010) The effect of combined antiretroviral therapy on the overall mortality of HIV-infected individuals. AIDS 24: 123–137.
24. Sterne JA, May M, Costagliola D, de Wolf F, Phillips AN, et al. (2009) Timing of initiation of antiretroviral therapy in AIDS-free HIV-1-infected patients: a collaborative analysis of 18 HIV cohort studies. Lancet 373: 1352–1363.
25. Biron KK (2006) Antiviral drugs for cytomegalovirus diseases. Antiviral Res 71: 154–163.

SCIENTIFIC REPORTS

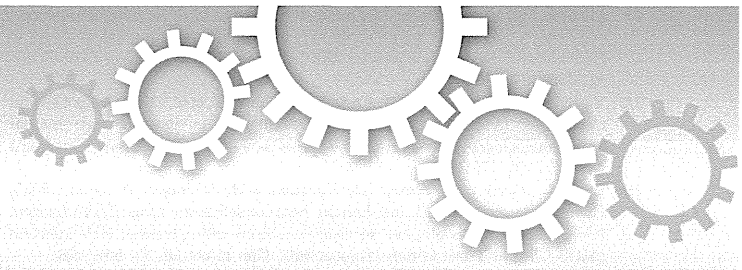

OPEN

SUBJECT AREAS:
INFECTION
HIV INFECTIONS
RETROVIRUS
VIRAL MEMBRANE FUSION

Received
12 April 2013

Accepted
24 July 2013

Published
8 August 2013

Correspondence and requests for materials should be addressed to H.G. (higatana@acc.ncgm.go.jp)

Arginine insertion and loss of N-linked glycosylation site in HIV-1 envelope V3 region confer CXCR4-tropism

Kiyoto Tsuchiya[1], Hirotaka Ode[2,3], Tsunefusa Hayashida[1,4], Junko Kakizawa[1], Hironori Sato[2], Shinichi Oka[1,4] & Hiroyuki Gatanaga[1,4]

[1]AIDS Clinical Center, National Center for Global Health and Medicine, 1-21-1 Toyama, Shinjuku-ku, Tokyo 162-8655, Japan, [2]Pathogen Genomics Center, National Institute of Infectious Diseases, 4-7-1 Gakuen, Musashimurayama-shi, Tokyo 208-0011, Japan, [3]Clinical Research Center, National Hospital Organization Nagoya Medical Center, 4-1-1 Sannomaru, Naka-ku, Nagoya 460-0001, Japan, [4]Center for AIDS Research, Kumamoto University, 2-2-1 Honjo, Chuo-ku, Kumamoto 860-0811, Japan.

The third variable region (V3) of HIV-1 envelope glycoprotein gp120 plays a key role in determination of viral coreceptor usage (tropism). However, which combinations of mutations in V3 confer a tropism shift is still unclear. A unique pattern of mutations in antiretroviral therapy-naive HIV-1 patient was observed associated with the HIV-1 tropism shift CCR5 to CXCR4. The insertion of arginine at position 11 and the loss of the N-linked glycosylation site were indispensable for acquiring pure CXCR4-tropism, which were confirmed by cell-cell fusion assay and phenotype analysis of recombinant HIV-1 variants. The same pattern of mutations in V3 and the associated tropism shift were identified in two of 53 other patients (3.8%) with $CD4^+$ cell count <200/mm^3. The combination of arginine insertion and loss of N-linked glycosylation site usually confers CXCR4-tropism. Awareness of this rule will help to confirm the tropism prediction from V3 sequences by conventional rules.

Since the introduction of maraviroc, a specific CCR5 antagonist, into clinical practice, scientific and clinical studies have focused on the coreceptor usage of human immunodeficiency virus type 1 (HIV-1)[1]. Evidence indicates the presence of a homogeneous population of predominantly CCR5-tropic variants[2,3] early in HIV-1 infection[4,5]. CXCR4-tropic variants[6,7], against which specific CCR5 antagonists are inefficient, can be distinguished from R5-tropic variants by their tendency for higher replication kinetics and a broader target cell range[8]. Their presence *in vivo* has been associated with accelerated fall in $CD4^+$ cell count and rapid disease progression[9,10]. CXCR4-tropic variants evolve from CCR5-tropic ones in the natural course of HIV-1 infection, though the exact mechanism of viral tropism evolution is not known yet. Long-term observation of natural course, which is indispensable for understanding the mechanism of tropism evolution, is usually difficult, because early use of antiretroviral therapy (ART) is highly recommended[11]. In this study, untreated natural course of one hemophiliac, who acquired HIV-1 infection through contaminated blood product before 1985 and exhibited slow disease progression, was followed until a rapid fall in $CD4^+$ cell count in 2007. The sequence change in the HIV-1 envelope (Env) glycoprotein gp120 V3 region (V3), the main determinant of HIV-1 tropism[12], was analyzed between 2003 and 2007. The results identified a unique change in 2007 associated with change in HIV-1 tropism. The same kind of sequence change in V3 was also identified in two other patients and in some of the registered sequences in the Los Alamos HIV sequence database.

Results

V3 sequence changes in Case 1. Case 1 was an ART-naive Japanese hemophiliac who acquired HIV-1 subtype B infection through contaminated blood product before 1985 and exhibited a slow disease progression. We reported previously the emergence of an escape mutation in HIV-1 Pol from cytotoxic T-lymphocyte (CTL) response in association with a mild increase in viral load in 1999 in this patient (KI-127)[13]. The HIV-1 viral load was steady around 10^4 copies/mL between 2002 and 2006 (Figure 1a). However, at the end of 2006, the viral load began to increase, coupled with a rapid fall in $CD4^+$ cell count. Since the emergence of CXCR4-tropic variants was suspected, changes in the V3 region were analyzed at five time points (June 2003, April 2006, and January, April, and November 2007) by sequencing 19–27 clones. Originally, most of the clones had identical or resembled V3

SCIENTIFIC REPORTS SREP-13-01550.3d 29/7/13 14:41:48

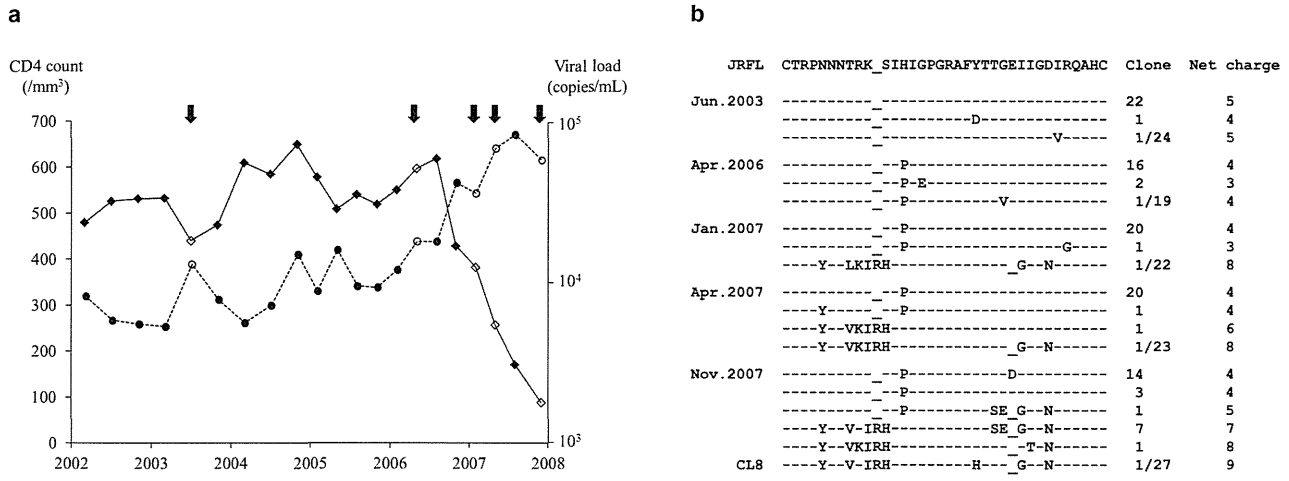

Figure 1 | (a). Clinical course of Case 1. The CD4$^+$ cell count (diamonds and solid lines) and HIV-1 load (circles and broken lines) from 2002 to 2008 are plotted. Arrows at the top indicate the five time points when V3 sequences were analyzed. Open diamonds and circles indicate the CD4$^+$ cell counts and HIV-1 loads at the same five time points. (b). V3 sequence changes in Case 1.Cloned sequences analyzed at the five time points are shown. The V3 sequence of HIV-1 JRFL is shown at the top column as a reference. Amino acids identical to those of HIV-1 JRFL are indicated as dashes. The numbers of clones harboring the corresponding V3 sequences are shown on the right.

sequences with CCR5-tropic HIV-1 JRFL (Figure 1b). Interestingly, a unique clone, harboring arginine insertion at position 11 of V3 (Ins11R), one amino acid deletion at position 25 (Del25), and other multiple amino acid substitutions, was identified at a frequency of 1/22 in January 2007, and the frequency of the same kind of the clones subsequently increased to 2/23 in April 2007, and 9/27 in November 2007, which was considered to be associated with the rapid fall in CD4$^+$ cell count.

Insertion and deletion confer CXCR4-tropism. In the next step, cell-cell fusion assay was performed to analyze the effect of the observed V3 changes on viral tropism, using Env-expressing 293 T cells and CD4$^+$ and CCR5$^+$/CXCR4$^+$ COS-7 cells. One V3 clone harboring Ins11R and Del25 identified in November 2007, named CL8-V3 (Figure 1b), was incorporated into JRFL Env-expressing plasmid. The cell-cell fusion assay demonstrated that CL8-V3 was purely CXCR4-tropic whereas JRFL was purely CCR5-tropic (Figure 2a). Ins11R occurred by the insertion of 'ACA' between 'G' and 'T' of 'AGT' at position 11 at nucleotide sequence level, and therefore, the substitution of serine (S) with histidine (H) at position 12 (S12H) was also associated with Ins11R in Case 1 ('AGT' → 'AGACAT' at nucleotide level; 'S' → 'RH' at amino acid level [Ins11R/S12H]). To identify the determinant of observed tropism change, the plasmids harboring Ins11R/S12H, Del25, and Ins11R/S12H/Del25 were also constructed using JRFL backbone. In the cell-cell fusion assay, Ins11R/S12H decreased CCR5-tropism of

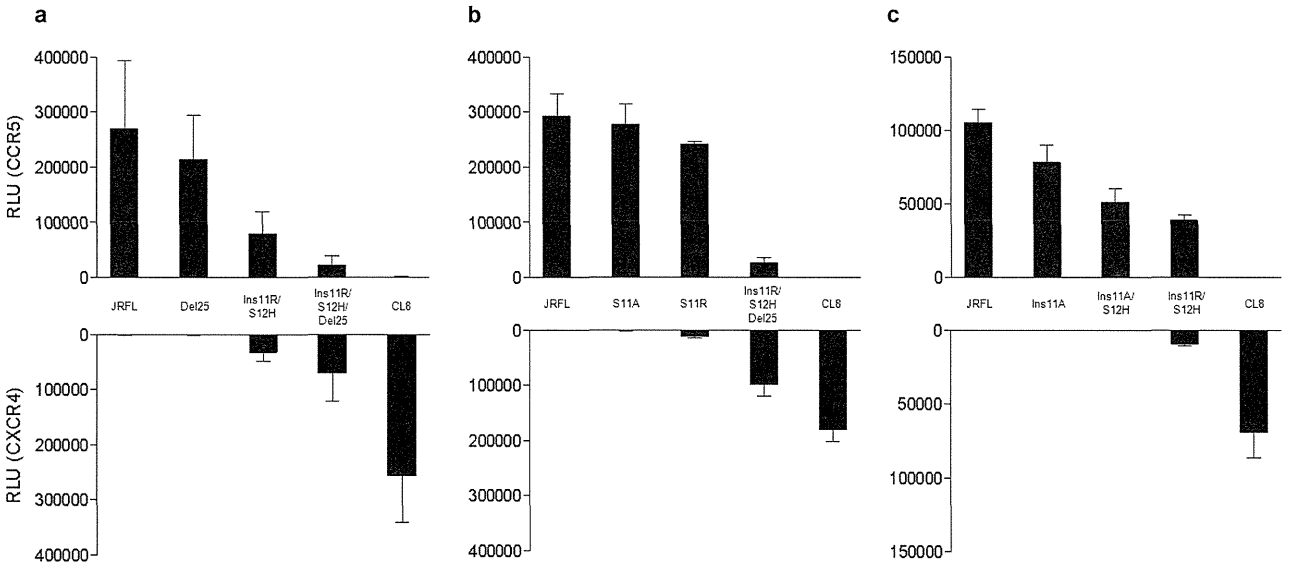

Figure 2 | Effect of Ins11R/S12H and Del25 in cell-cell fusion assay (a). Cell-cell fusion assay was performed using Env-expressing 293 T cells and CD4$^+$ and CCR5$^+$/CXCR4$^+$ COS-7 cells. Data are mean±SD values in relative luminescent unit (RLU) of six experiments (performed in duplicate and repeated three times). Analysis of two elements of Ins11R in cell-cell fusion assay (b and c). Effects of placing R at position 11 (b) and one amino acid elongation of V3 (c) were analyzed. Cell-cell fusion assay was performed using Env-expressing 293 T cells and CD4$^+$ and CCR5$^+$/CXCR4$^+$ COS-7 cells. Data are mean±SD values in relative luminescent unit (RLU) of six experiments (performed in duplicate and repeated three times).

JRFL-V3 and conferred CXCR4-tropism, resulting in dual-tropic (Ins11R/S12H vs. JRFL). Del25 further decreased the CCR5-tropism of Ins11R/S12H-V3 and increased CXCR4-tropism (Ins11R/S12H/Del25 vs Ins11R/S12H), though Del25 alone did not significantly change the JRFL-V3 tropism (Del25 vs JRFL). Considered together, the results suggest that Ins11R/S12H is indispensable for CXCR4-tropism of CL8-V3 and that Del25 strengthened the CXCR4-tropism in the presence of Ins11R/S12H. However, their combination was not enough to confer JRFL-V3 pure CXCR4-tropism (Ins11R/S12H/Del25-V3-expressing 293 T cells still fused with $CD4^+/CCR5^+$ COS-7 cells at low level), and some other mutations were necessary for pure CXCR4-tropism of CL8-V3.

Which is important, substitution or elongation? The above results suggested that Ins11R/S12H was indispensable for CXCR4-tropism of CL8-V3. According to the 11/25 rule, a basic amino acid residue (R or lysine [K]) at either position 11 or 25 of V3 is associated with CXCR4-tropism, whereas acidic or neutral amino acid residues at these positions are associated with CCR5-tropism[12,14,15]. Ins11R/S12H has two elements: one is to place R at position 11 and the other is one amino acid elongation of V3. To determine whether positioning R at 11 is sufficient for conferring CXCR4-tropism or whether V3 elongation is also necessary for this process, S at position 11 of JRFL-V3 was substituted with R (S11R) and alanine (A) (S11A) as reference. However, both substitutions did not alter the pure CCR5-tropism of JRFL (Figure 2b), indicating that not only R at position 11 but also one amino acid elongation was indispensable for dual tropism caused by Ins11R/S12H.

Is one amino acid elongation sufficient to induce CXCR4-tropism or is positioning R at 11 is also necessary? To answer this question, two V3-expressing plasmids were constructed; one harbored Ins11A only and the other harbored Ins11A and S12H (Ins11A/S12H). The cell-cell fusion assay indicated that Ins11A decreased and Ins11A/S12H further decreased infectivity with CCR5 though neither of them conferred CXCR4-tropism (Figure 2c). These results indicate that not only one amino acid elongation of V3 but also positioning R at 11 is indispensable for dual tropism caused by Ins11R/S12H.

Effect of net charge of V3. Ins11R/S12H conferred CXCR4-tropism and Del25 strengthened it. However, Ins11R/S12H/Del25-V3 was still dual-tropic, though CL8-V3 was purely CXCR-4 tropic. The next question was which mutation is necessary for Ins11R/S12H/Del25-V3 to become purely CXCR4-tropic, like CL8-V3 (to lose CCR5-tropism)? There are six amino acid substitutions in CL8-V3 (substitution of asparagine [N] with tyrosine [Y] at position 5 [N5Y], substitution of threonine [T] with valine [V] at position 8 [T8V], substitution of K with isoleucine [I] at position 10 [K10I], substitution of Y with H at position 22 [Y22H], substitution of V with glycine [G] at position 26 [V26G], and substitution of aspartic acid [D] with N at position 29 [D29N]), compared with Ins11R/S12H/Del25-V3. According to the net charge rule, the higher net charge of V3 is associated with CXCR4-tropism when calculated by subtracting the number of negatively charged amino acid residues (D and glutamic acid [E]) from the number of positively charged ones (K and R)[12,14]. D29N was the only amino acid substitution that increased the net charge of V3 among the six amino acid substitutions described above. Therefore, we analyzed the effect of D29N by adding D29N to Ins11R/S12H/Del25-V3 (Ins11R/S12H/Del25/D29N) and reverting it in CL8-V3 (CL8/N29D). In the cell-cell fusion assay, D29N reduced CCR5-tropism of Ins11R/S12H/Del25-V3 though it remained dual-tropic (Ins11R/S12H/Del25/D29N vs Ins11R/S12H/Del25), and the reversion of D29N did not change CL8-V3 tropism (CL8/N29D vs CL8) (see Supplementary Figure S1). These results indicate that D29N does not cause tropism difference between Ins11R/S12H/Del25-V3 and CL8-V3, indicating that the net charge rule did not work well.

***In silico* prediction of the effect of substitutions.** Adding D29N failed to alter the tropism of Ins11R/S12H/Del25-V3 from dual-tropic to purely CXCR4-tropic. There were five other amino acid substitutions between Ins11R/S12H/Del25-V3 and CL8-V3. Because the V3 conformation is important for coreceptor interactions[16] and because conformation of V3 loop is sensitive to V3 mutations[17,18], we examined how these V3 mutations could influence conformation of V3 in solution using molecular dynamics (MD) simulation[19]. In our MD simulation study, V3-loops of JRFL and Del25 (both CCR5-tropic) were placed in the opposite direction from the β20-β21 loop (Figure 3a), while CL8-V3 loop (CXCR4-tropic) was closed to and in the same direction with the β20-β21 loop (Figure 3c). The results were consistent with those obtained with $gp120_{LAI}$ recombinant outer domains containing CCR5-tropic and CXCR4-tropic V3 loop, respectively[17,18]. The loops of dual-tropic Ins11R/S12H-V3 and Ins11R/S12H/Del25 were located between Del25-V3 and CL8-V3 (Figure 3b). In fact, when the structural differences at the tip of the V3 tip region, i.e., the 'GPGR' amino acid residues were quantitatively measured with the root mean square deviation (RMSD) of the main chain[17], CL8-V3 was found to be located far from the loop of JRFL-V3 and Del25-V3, while those of Ins11R/S12H-V3 and Ins11R/S12H/Del25-V3 were between them (Table 1). These results suggest that our MD simulation could predict the V3 tropism based on the magnitude of the RMSD values of the V3 loop tip. In the next step, each of the six amino acid substitutions of CL8-V3 was incorporated into Ins11R/S12H/Del25-V3, and the location and conformation of the constructed loop was analyzed. When D29N was incorporated, the RMSD from JRFL-V3 decreased and that from CL8-V3 increased (Table 2), and the loop orientation was still similar to that of Ins11R/S12H/Del25 (Figure 3d), suggesting that D29N does not seem to change the tropism, compatible with the results of the cell-cell fusion assay (see Supplementary Figure S1). Among other single amino acid substitutions, only T8V was found to increase the RMSD from JRFL-V3 and decrease that from CL8-V3 (Table 2), and caused a positional shift of the V3 resembling that of the CL8-V3 (Figure 3e). N5Y did not change the orientation of the V3 loop (see Supplementary Figure S2a) though the RMSD from CL8-V3 increased and that from JRFL-V3 decreased (Table 2). K10I, Y22H, and V26G decreased the RMSD from JRFL-V3 and increased that from CL8-V3 (Table 2), and the V3 loop orientation was distinct from both Ins11R/S12H/Del25-V3 and CL8-V3 (see Supplementary Figure S2b, S2c, and S2d). These results suggest that among the six amino acid substitutions, T8V has the greatest impact on the tropism shift toward CXCR4-tropic.

Impact of T8V. Our *in silico* modeling predicted that T8V could alter the tropism of Ins11R/S12H/Del25-V3. In the next series of experiments, we incorporated T8V into JRFL-V3 (JRFL/T8V) and Ins11R/S12H/Del25-V3 (Ins11R/S12H/Del25/T8V), and analyzed the effect of such incorporation on their tropism using the cell-cell fusion assay. The incorporation of T8V into JRFL-V3 increased CCR5-tropism though it did not confer CXCR4-tropism (Figure 4a and 4b). However, T8V abrogated CCR5-tropism of Ins11R/S12H/Del25-V3 and converted it to purely CXCR4-tropic, although it did not increase CXCR4-tropism and Ins11R/S12H/Del25/T8V-V3 still had smaller CXCR4-tropism than CL8-V3 (Figure 4a). The combination of Ins11R/S12H/T8V was sufficient to confer CXCR4-tropism, although Del25/T8V did not (Figure 4b). T8V breaks the N-linked glycosylation motif 'NXT' at position 6–8 of V3, the loss of which was reported with tropism shift towards CXCR4-tropic[20,21]. Our results indicated that T8V was indispensable for pure CXCR4-tropism of CL8, which seemed to support the previous findings of the importance of the loss of N-linked glycosylation motif for CXCR4-tropism. The loss of the glycan moiety in V3 stem might lead to change gp120 interaction surface for coreceptor binding and influence coreceptor

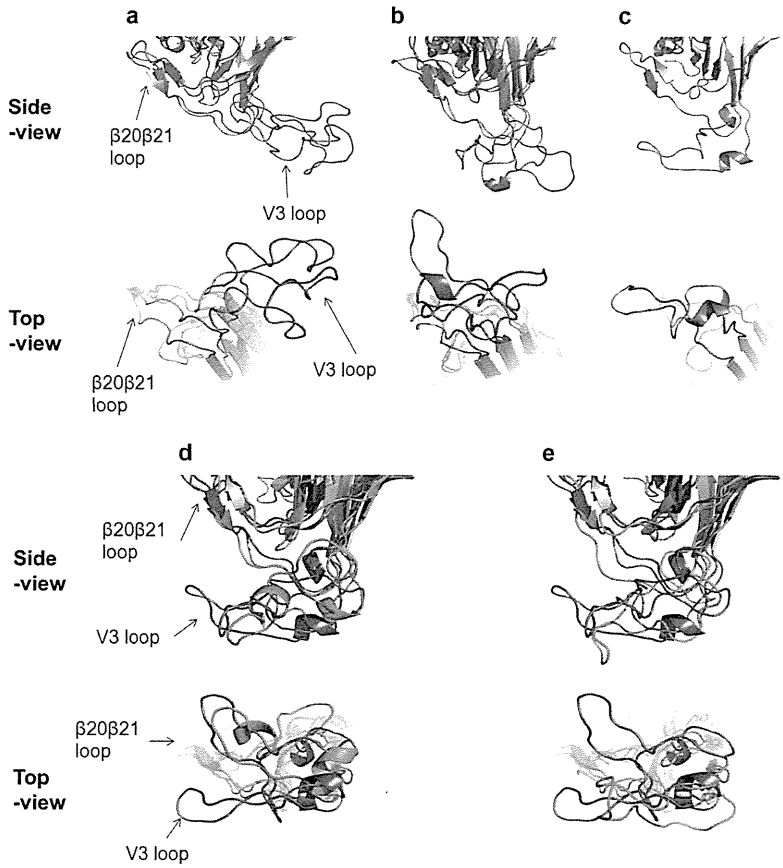

Figure 3 | Structural models of V3 loops on HIV-1 gp120 outer domains (a, b and c). MD simulations were performed for the HIV-1 JRFL gp120 outer domain with various V3 loops for CCR5 (a), dual (b), and CXCR4 (c) tropism. The most frequently appeared structures during 5–10 ns of MD simulations were extracted, and the top and side views of the structures around V3 loops are highlighted. (a) JRFL (gray) and Del25 (navy). (b) Ins11R/S12H/Del25 (gray) and Ins11R/S12H (navy). (c) CL8 (gray). Structural models of V3 loops of Ins11R/S12H/Del25-derived mutants (d and e). MD simulations were performed for the HIV-1 Ins11R/S12H/Del25 gp120 outer domain with D29N (d) or T8V (e) substitution in V3 loop. The most frequently appeared structures during 5–10 ns of MD simulations were extracted and superimposed with those of Ins11R/S12H/Del25 and CL8. (d) Superimposition of D29N (green), Ins11R/S12H/Del25 (gray), and CL8 (navy). (e) Superimposition of Ins11R/S12H/Del25/T8V (green), Ins11R/S12H/Del25 (gray), and CL8 (navy). Top and side views of the structures around V3 loops are shown.

tropism. However, available structural information was against this possibility, because the glycosylation site was exposed toward an opposite direction from the putative coreceptor binding site on V3[16,22,23]. Accordingly, presence or absence of the glycan moiety in V3 stem did not cause significant differences in V3 configuration in our MD simulation system[17,24]. Probably, amino acid substitution itself altered V3 configuration and coreceptor tropism.

Table 1 | Overall structural differences between the two V3 loop tips of various HIV-1 variants

	RMSD (Å)*			
ID of V3	JRFL	Del25	Ins11R/S12H	Ins11R/S12H/Del25
Del25	13.8	-	-	-
Ins11R/S12H	17.4	8.6	-	-
Ins11R/S12H/Del25	29.4	28.7	23.6	-
CL8	38.9	37.5	33.1	14.2

*RMSD values of the main chain atoms at V3 tips (GPGR) of two gp120 outer domain models from MD simulations. A smaller RMSD value means a closer conformation between two gp120s.

GHOST cell infection assay. Our cell-cell fusion assay indicated that Ins11R/S12H and T8V were indispensable for pure CXCR4-tropism of CL8. The next series of experiments were designed to confirm the findings using HIV-1 infection assay in GHOST cells[25,26]. HIV-1 JRFL and the recombinant HIV-1 variants harboring Del25-V3 and T8V-V3 had the same level of CCR5-tropism, although none could infect CXCR4$^+$ GHOST cells (Figure 4c). In comparison, Ins11R/S12H-V3- and Ins11R/S12H/Del25-V3-harboring variants had lower levels of CCR5-tropism. The latter variant, but not the former, infected CXCR4$^+$ GHOST cells though at low level. The Ins11R/S12H/Del25/T8V-V3-harboring variant lost the CCR5-tropism and acquired CXCR4-tropism, although the level of CXCR4-tropism was still lower than those of CL8-V3-harboring variant and HIV-1 NL4-3 (a CXCR4-tropic experimental strain). These results were compatible with the abovementioned results of the cell-cell fusion assay, though the CCR5-tropism of Ins11R/S12H/Del25-V3 seemed stronger in the cell infection assay. Dual-tropic Ins11R/S12H/Del25-V3 might have decreased susceptibility to AMD3100 used in the CCR5$^+$ GHOST Hi5 assay compared with pure CXCR4-tropic CL8-V3 and NL4-3-V3.

Same V3 pattern in two other cases. The analysis of V3 sequence changes in Case 1 demonstrated that Ins11R and the loss of N-linked

Table 2 | Effect of a single amino acid substitution on overall structure of the gp120 V3 tip

ID of V3	Added mutations*	RMSD (Å)† JRFL	RMSD (Å)† CL8
Ins11R/S12H/Del25	None	29.4	14.2
Ins11R/S12H/Del25/N5Y	N5Y	32.5	14.1
Ins11R/S12H/Del25/T8V	T8V	33.6	12.6
Ins11R/S12H/Del25/K10I	K10I	26.3	39.4
Ins11R/S12H/Del25/Y22H	Y22H	28.6	27.0
Ins11R/S12H/Del25/V26G	V26G	28.4	19.6
Ins11R/S12H/Del25/D29N	D29N	28.4	17.0

*Added amino acid substitution in the V3 loop of the Ins11R/S12H/Del25 gp120.
†RMSD values of the main chain atoms at V3 tips (GPGR) of two gp120 outer domain models from MD simulations.

glycosylation site indispensably contribute to a shift toward CXCR4-tropism. To determine whether this finding was true only in Case 1 or could be generalized to other cases, HIV-1 subtype B V3 sequences were analyzed in 53 other treatment-naïve patients with $CD4^+$ cell count $< 200/mm^3$. The same pattern of mutations was identified in two cases (3.8%). In one case (Case 2), four of twenty analyzed sub-clones of V3 sequences harbored Ins11R associated with S12H, Del25, and N6A resulting in the loss of N-linked glycosylation site, compared with JRFL-V3 (Figure 5). In the other case (Case 3), three of twenty-two sub-clones harbored Ins11R associated with S11R, Del25, and T8V, resulting in the loss of N-linked glycosylation site. To delineate the tropism of the V3 abovementioned clones, two V3 clones in each case, one harboring Ins11R and the loss of N-linked glycosylation site (KF6 in Case 2, T16 in Case 3 [see Figure 5]) and the other harboring none of them (KF8 in Case 2, T02 in Case 3 [see Figure 5]), was incorporated into JRFL Env-expressing plasmid. As expected, cell-cell fusion assay indicated that the clones harboring Ins11R and the loss of N-linked glycosylation site (KF6 and T16) were purely CXCR4-tropic, although the clones harboring none of them (KF8 and T02) were purely CCR5-tropic (Figure 6a and 6b). The results of the GHOST cell infection assay using V3-incorporated HIV-1 JRFL (Figure 6c) were similar to those of the cell-cell fusion assay. Accordingly, it was concluded that the findings of the indispensability of Ins11R and the loss of N-linked glycosylation site for CXCR4-tropism were not only true in Case 1 but also in other cases.

Discussion

The phenotypic assay Trofile™ (Monogram Bioscience, South San Francisco, CA), which is based on recombinant virus technology, has been the most widely used diagnostic test for the detection of CXCR4-tropic HIV-1 variants[27]. However, this method has logistical and technical limitations that make it far from convenient as a diagnostic test in clinical practice. Genotypic methods based on V3 sequence represent a more feasible alternative[28] and are progressively replacing phenotypic assays, though their clinical use requires good genotypic-phenotypic correlations. The 11/25 rule and the net charge rule were proposed for the tropism prediction from V3 sequence[12,14,15], although they show only a moderate correlation with the results of phenotypic assays[12,15,28]. The results of specific genotypic tools, such as geno2pheno (Max-Planck Institute, Munich, Germany)[29,30] and position-specific scoring matrix (PSSM)[31,32] are comparable to those of phenotypic assays, suggesting that there should be some more genetic determinations for viral tropism. In this study, we successfully demonstrated two rules other than the 11/25 rule and the net charge rule on the association with CXCR4-tropic variants. One was that R insertion at position 11 of V3, not just placing R at position 11 but also one amino acid elongation, strongly shifted the HIV-1 tropism towards CXCR4-tropic. The other was that the loss of N-linked glycosylation site in V3 also shifted viral tropism towards CXCR4-tropic, which was previously described in some reports[20,21]. In the V3 analysis in our index case, R insertion at position 11 conferred dual-tropism to originally CCR5-tropic V3, and the loss of N-linked glycosylation site altered it totally CXCR4-tropic (see Supplementary Figure S3). We identified these mutation patterns not only in the index case but also in two other cases. When we surveyed V3 sequences with tropism confirmed by phenotypic assay registered at the Los Alamos HIV sequence database (Los Alamos National laboratory, Los Alamos, NM) (http://www.hiv.lanl.gov. as of September 25, 2012), 28 sequences had R insertion at position 11; 7 of 199 (3.5%) CXCR4-tropic, 14 of 513

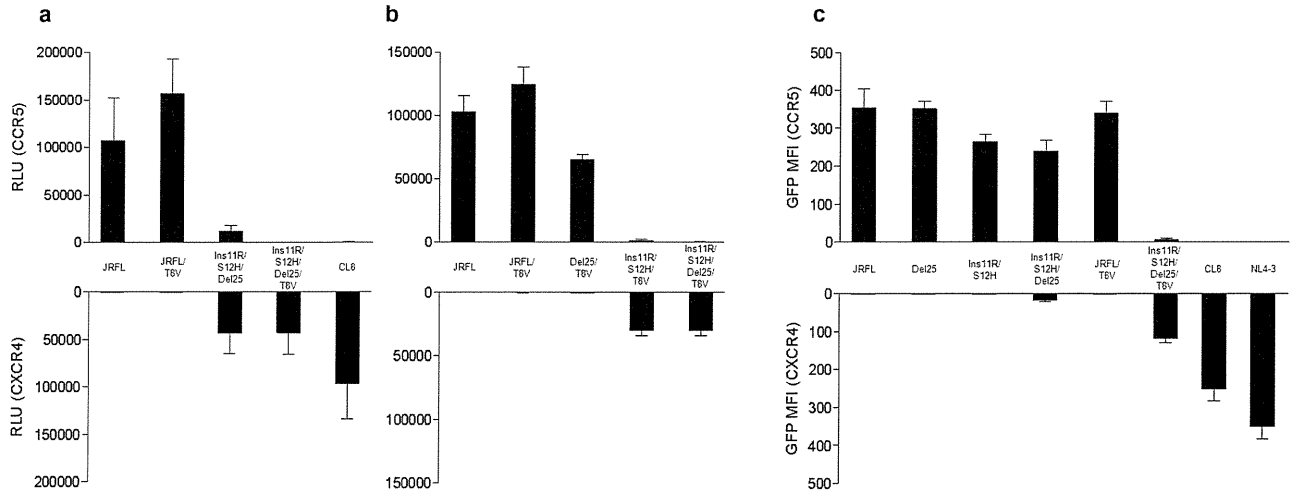

Figure 4 | Effects of T8V in cell-cell fusion assay (a and b). The effects of T8V were analyzed in combination with Ins11R/S12H/Del25 (a), and Del25 and Ins11R/S12H (b). Cell-cell fusion assay was performed using Env-expressing 293 T cells and $CD4^+$ and $CCR5^+$/$CXCR4^+$ COS-7 cells. Data are mean±SD values in relative luminescent unit (RLU) of six experiments (performed in duplicate and repeated three times). Tropism of recombinant HIV-1 variants harboring mutations identified in Case 1 (c). Tropism of HIV-1 variants was assessed in $CCR5^+$ GHOST Hi5 and $CXCR4^+$ GHOST CXCR4 cells. The mean fluorescent intensity (MFI) of infected cells expressing green fluorescent protein (GFP) was measured. Data are mean±SD values of six experiments (performed in duplicate and repeated three times).

		JRFL CTRPNNNTRK_SIHIGPGRAFYTTGEIIGDIRQAHC	Clone	Net charge
Case2	KF8	----------_G--M------F-DN_------K---	12	6
		---------R_G--M------F-DN_------K---	2	6
		----------_G--M---G--F-DN_------K---	1	5
		----------_G--M------F-DN_------K-Y-	1	5
	KF6	-----AI-K-RHF----------NN_KV----K---	2	10
		-----AI-KRRHF----------NK_-V----K---	1	9
		-----AI-K-RHF----------N_KV----K---	1/20	10
Case3	T02	----------_----------FA-D_---N--K-Y-	16	6
		----------_----------FA-D_------K-Y-	2	5
		----S-----_----------FA-D_------K-Y-	1	5
	T16	------KVIRRR---------VA-D_TT----K-Y-	3/22	7

Figure 5 | Cloned V3 sequences in Cases 2 and 3. The V3 sequence of HIV-1 JRFL is shown at the top column as a reference. Amino acids identical to those of HIV-1 JRFL are indicated as dashes. The numbers of clones harboring the corresponding V3 sequences are shown on the right.

(2.7%) dual-tropic, and 7 of 3301 (0.2%) CCR5-tropic sequences. Their frequency was significantly higher in CXCR4-tropic and dual-tropic sequences than CXCR5-tropic ones ($p < 0.0001$; Chi-square test). (All of the 7 CCR5-tropic sequences with R insertion at position 11 were sub-clones derived from one pair of a transmitter mother and her transmitted child[33], and the sequences were so unique that it was actually difficult to determine the exact site of one amino acid insertion). Interestingly, all of the 28 V3 sequences with R insertion at position 11, had lost the N-linked glycosylation site and had one amino acid deletion in the C-terminal half of V3 (one amino acid deletion at position 24 or 25 in 18 sequences [64.3%]), similar to our three cases. No other amino acid elongation patterns were found in the N-terminal half of V3 in the Los Alamos database. There were 3,301 CCR5-tropic V3 sequences registered in the database. Among them, 18 sequences had a basic amino acid residue at position 11 and therefore they were misjudged as CXCR4-tropic by the 11/25 rule. Only 7 of them had R insertion and the other 11 were recognized as CCR5-tropic by our rules. Therefore using our rules increased the specificity from 99.5% [(3,301–18)/3,301] to 99.8% [(3,301–7)/3,301] in identifying CXCR4- or dual-tropic V3 sequences in the Los Alamos database.

Considered together, amino acid elongation may be a rare event, but R insertion at position 11 sometimes occurs. The occurrence of such insertion seems to be always accompanied by loss of the N-linked glycosylation site and deletion of one amino acid in the C-terminal half of V3. The combination of these mutations usually confers CXCR4-tropism. Awareness of this rule will help to confirm the tropism prediction from V3 sequences by conventional rules.

Methods

Patients. Case 1 was an ART-naive Japanese hemophiliac who acquired HIV-1 subtype B infection through contaminated blood product before 1985 and exhibited slow disease progression, as described previously (KI-127)[13]. The study also included 53 other treatment-naïve HIV-1 subtype B-infected patients with $CD4^+$ cell count < 200/mm^3, who were newly diagnosed in 2008. The ethics committee of The National Center for Global Health and Medicine approved the study and all participants provided written informed consent.

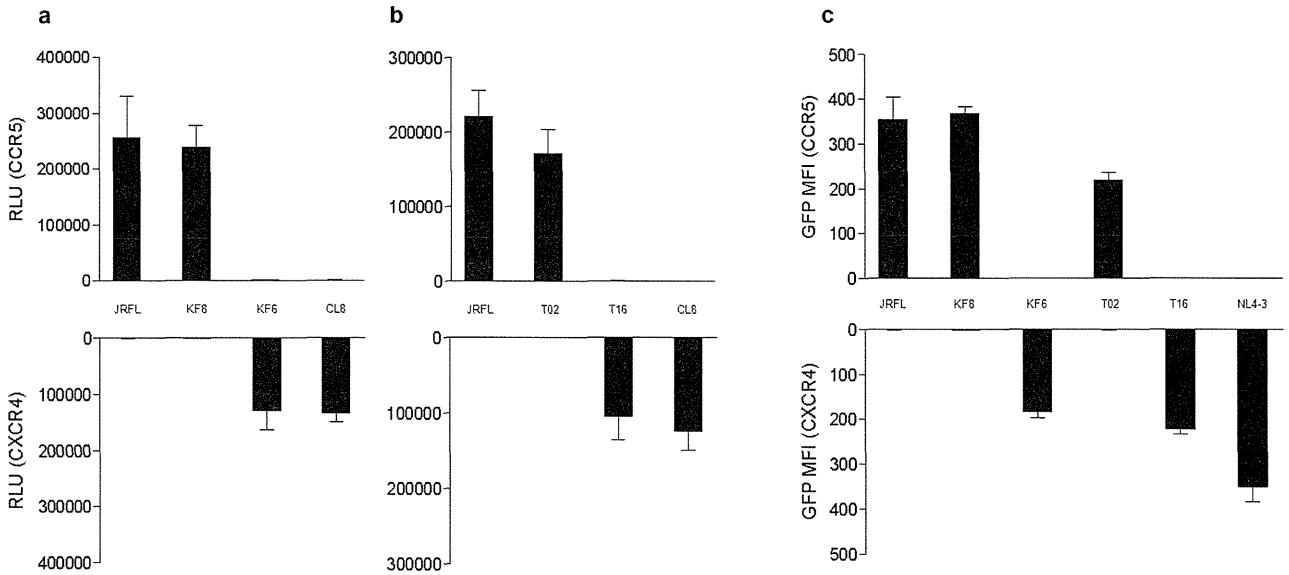

Figure 6 | Tropism of cloned V3 incorporated into JRFL gp120 backbone (a and b). Two distinct V3 clones from each of Case 2 (a) and Case 3 (b) were analyzed with the reference of JRFL-V3 and CL8-V3. Cell-cell fusion assay was performed using Env-expressing 293T cells and $CD4^+$ and $CCR5^+$/$CXCR4^+$ COS-7 cells. Data are mean±SD values in relative luminescent unit (RLU) of six experiments (performed in duplicate and repeated three times). Tropism of recombinant HIV-1 variants harboring V3 sequences derived from Cases 2 and 3 (c). Tropism of HIV-1 variants was assessed in $CCR5^+$ GHOST Hi5 and $CXCR4^+$ GHOST CXCR4 cells. The mean fluorescent intensity (MFI) of infected cells expressing green fluorescent protein (GFP) was measured. Data are mean±SD values of six experiments (performed in duplicate and repeated three times).

Cells. The 293 T and COS-7 cells were cultured in Dulbecco's modified Eagle's medium (DMEM; Gibco, Grand Island, NY) with 10% fetal bovine serum (FBS; Equitech-Bio, Kerrville, TX). Parental GHOST cells[34] were cultured in DMEM supplemented with 10% FBS, 500 μg/ml G418 and 100 μg/ml hygromycin B. CCR5$^+$ GHOST Hi5 and CXCR4$^+$ GHOST CXCR4 cells[34] were cultured in DMEM supplemented with 10% FBS, 500 μg/ml G418, 100 μg/ml hygromycin B and 1 μg/ml puromycin.

Amplification, cloning and sequencing of Env V3 region. Total RNA was extracted from 200 μl of plasma using High Pure Viral RNA Kit (Roche, Indianapolis, IN) according to the instructions supplied by the manufacturer. HIV-1 cDNA was obtained by reverse transcriptase-polymerase chain reaction (RT-PCR) using the One Step RNA PCR kit (TaKaRa Bio, Kyoto, Japan). The DNA fragments were amplified by using the Ex Taq Hot Start Version (TaKaRa Bio) with the primer sets as follows. The Env fragment containing V3 region was amplified by RT-PCR with primers of C2 (5′ - AATGTCAGCACAGTACAATGTACAC - 3′) and C3 (5′ - ACAATTTCTGG GTCCCCTCCTGAGGA - 3′). S1 (5′ - ATGGAATTAGGCCAGTAGT - 3′) and A1 (5′ - CTCTTAATTTTATAACTATC - 3′) primer sets were used for nested PCR. The amplified PCR products were purified using QIAquick PCR purification kit (Qiagen, Valencia, CA) and cloned by using the TOPO TA Cloning Kit (Invitrogen, Carlsbad, CA) according to the protocol provided by the manufacturer. At least 19 colonies were selected, inoculated into 4 ml of L broth, and incubated at 37°C overnight under vigorous agitation. In the next step, plasmids were isolated by using the QIAprep Spin Miniprep Kit (Qiagen). The purified plasmids were sequenced by using the ABI BigDye Terminator v3.1 Cycle Sequencing Ready Reaction Kit (Applied Biosystems, Foster City, CA) and processed with an automated ABI 3730 DNA Analyzer (Applied Biosystems).

Plasmid construction. The pcDNA6.2-CCR5 and pcDNA6.2-HIV-tat plasmids were constructed as described previously[35]. Briefly, the entire human CCR5 gene including a stop codon was amplified using pZeoSV-CCR5[36] as a template. The PCR product was ligated into pcDNA6.2/cLumio-DEST vector (Invitrogen), cloned using the method recommended by the manufacture, and termed as pcDNA6.2-CCR5. The CD4 expression vector (pcDNA6.2-CD4) and CXCR4 expression vector (pcDNA6.2-CXCR4) were generated using the same method. The CCR5-tropic HIV-1 JRFL[37] Env expression vector (pCXN-JRenv) and pLTR-LucE were used as described previously[35]. The full length Env and part of the Nef encoding regions of the HIV-1 genome was amplified using pHIV-1 JRFL. The PCR product was ligated into pGEM-T Easy Vector System (Promega, Madison, WI), cloned using the protocol supplied by the manufacturer, and termed as pGEM-T Easy-Env. Amino acid substitutions, insertion and deletion were introduced into the V3 region of pGEM-T Easy-Env using the Quikchange Site-directed Mutagenesis Kit (Stratagene, La Jolla, CA) and applying the protocols supplied by the manufacturer. The V3 regions of pGEM-T Easy-Env containing mutations were digested with *Stu*I and *Xho*I, and the obtained fragments were introduced into pCXN-JRenv or pHIV-1 JRFL.

Cell-cell fusion assay. The assay was conducted as described in detail previously[35]. Briefly, the JRFL Env expression vector (WT or mutant) and Tat expression vector (0.5 μg each) were cotransfected into 293 T cells (2×10^5) using Lipofectamine 2000 (Invitrogen), while the CD4, CCR5 or CXCR4 expression vector and a reporter (luciferase) gene containing plasmid, pLTR-LucE (0.5 μg each) were cotransfected into COS-7 cells (2×10^5). On the next day, both cotransfected cells were harvested and mixed in a well of 96-well plates (2×10^4 cells each). The cotransfected cells were incubated further for 6 hrs and the luciferase activity in each well was detected using Bright-Glo Luciferase Assay System (Promega) and its luminescence level was measured using Wallac ARVO Sx 1420 multilabel counter (Perkin-Elmer, Waltham, MA).

MD simulation. MD simulation of gp120 outer domain containing V3 loop was performed as described previously[17,18] with some modifications. Initially, the gp120 outer domain structures with various V3 elements were constructed by homology modeling[38,39] using the Molecular Operating Environment (MOE) ver. 2008.10 (Chemical Computing Group Inc., Montreal, Quebec, Canada), as described previously[17,18]. As a modeling template, we used the crystal structure of HIV-1 gp120 containing the entire V3 element (PDB code: 2B4C)[19]. Subsequently, MD simulations were performed for individual models using the SANDER module in the AMBER 9 program package[40,41]. Heating calculations were achieved for 100 picoseconds until 310 K and MD simulations were subsequently executed at 310 K for 10 nanoseconds. The time step was set to 2.0 femtoseconds. The AMBER ff03ua force field[42] and the GB implicit solvent function by Hawkins, Cramer, and Truhlar[43,44] were applied. The "no cutoff" calculation was applied for the non-bonded energy calculation. In this study, we analyzed most frequently observed conformation among 5,000 snapshots obtained from 5.0–10.0 ns of MD simulation, which was selected by the Bayesian clustering algorithm[45].

Calculation of the RMSD. We compared the orientation of V3 loop between two gp120 outer domain models by the following procedure. We first superimposed two models by coordinating main chain atoms (N, Cα, and C) in amino acid residues other than those in the V3 loop using PyMOL ver. 0.99 rc6 (Schrödinger LLC, Portland, OR, http://www.pymol.org/). Subsequently, the RMSD values for the V3 loop tip (GPGR) between the two models were calculated using the coordinates of the main chain atoms using the in-house program.

Viral tropism assay. The wild type CCR5-tropic HIV-1 strain, pHIV-1 JRFL, CXCR4-tropic HIV-1 strain, pHIV-1 NL4-3[46], and each pHIV-1 JRFL Env derived from mutations containing the V3 region of pGEM-T Easy-Env were transfected into 293 T cells with Lipofectamine 2000 (Invitrogen), and the obtained infectious clonal viruses were harvested 48 hrs after transfection and stored at −80°C until use. The GHOST cell infection assay[25,47] was performed by incubating 1 ml containing 20 ng of p24 antigen of each virus with GHOST cells (2×10^4). Parental GHOST, CCR5$^+$ GHOST Hi5, and CXCR4$^+$ GHOST CXCR4 cells were infected for 72 hrs and then harvested. The mean fluorescent intensity (MFI) of infected cells expressing green fluorescent protein (GFP) was measured on a flow cytometer (FACSCalibur; BD Bioscience, San Jose, CA). GHOST cells express low levels of CXCR4 and therefore infection of GHOST Hi5 alone was performed in presence of the CXCR4 antagonist AMD3100 (Sigma-Aldrich, St. Louis, MO) at dose of 1 μM.

1. Parra, J. *et al.* Clinical utility of maraviroc. *Clin. Drug Invest.* **31**, 527–542 (2011).
2. Alkhatib, G. *et al.* CC CKR5: a RNATES, MIP-1α, MIP-1β receptor as a fusion cofactor for macrophage-tropic HIV-1. *Science* **272**, 1955–1958 (1996).
3. Dragic, T. *et al.* HIV-1 entry into CD4+ cells is mediated by the chemokine receptor CC-CKR-5. *Nature* **381**, 667–673 (1996).
4. van't Wout, A. B. *et al.* Macrophage-tropic variant initiate human immunodeficiency virus type 1 infection after sexual, parenteral and vertical transmission. *J. Clin. Invest.* **94**, 2060–2067 (1994).
5. Zhu, T. *et al.* Genotypic and phenotypic characterization of HIV-1 in patients with primary infection. *Science* **261**, 1179–1181 (1993).
6. Björndal, A. *et al.* Coreceptor usage of primary human immunodeficiency virus type 1 isolates varies according to biological phenotype. *J. Virol.* **71**, 7478–7487 (1997).
7. Scarlatti, G. *et al.* In vivo evolution of HIV-1 co-receptor usage and sensitivity to chemokine mediated suppression. *Nat. Med.* **3**, 1259–1265 (1997).
8. Blaak, H. *et al.* In vivo HIV-1 infection of CD45RA+ CD4+ T cells is established primarily by syncytium-inducing variants and correlates with the rate of CD4+ T cell decline. *Proc. Natl. Acad. Sci. U. S. A.* **97**, 1269–1274 (2000).
9. Connor, R. I., Sheridan, K. E., Ceradini, D., Choe, S. & Landau, N. R. Change in copeceptor use correlates with disease progression in HIV-1-infected individuals. *J. Exp. Med.* **185**, 621–628 (1997).
10. Koot, M. *et al.* Prognostic value of human immunodeficiency virus type 1 biological phenotype for rate of CD4+ cell depletion and progression to AIDS. *Ann. Intern. Med.* **118**, 681–688 (1993).
11. The HHS Panel on Antiretroviral Guidelines for Adults and Adolescents. Guidelines for the Use of Antiretroviral Agents in HIV-1-Infected Adults and Adolescents. *U.S. Department of Health and Human Services* (2011).
12. Poveda, E. *et al.* Genotype determination of HIV tropism – clinical and methodological recommendations to guide the therapeutic use of CCR5 antagonists. *AIDS Rev.* **12**, 135–148 (2010).
13. Kawashima, Y. *et al.* Long-term control of HIV-1 in hemophiliacs carrying slow-progressing allele HLA-B*5101. *J. Virol.* **84**, 7151–7160 (2010).
14. Delobel, P. *et al.* Population-based sequencing of the V3 region of env for predicting the coreceptor usage of human immunodeficiency virus type 1 quasispecies. *J. Clin. Mcirob.* **45**, 1572–1580 (2007).
15. Vandekerckhove, L. P. *et al.* European guidelines on the clinical management of HIV-1 tropism testing. *Lancet Infect. Dis.* **11**, 394–407 (2011).
16. Huang, C. C. *et al.* Structures of the CCR5 N terminus and of a tyrosine-sulfated antibody with HIV-1 gp120 and CD4. *Science* **317**, 1930–1934 (2007).
17. Yokoyama, M., Naganawa, S., Yoshimura, K., Matsushita, S. & Sato, H. Structural dynamics of HIV-1 envelope gp120 outer domain with V3 loop. *PLoS One* **7**, e37530 (2012).
18. Naganawa, S. *et al.* Net positive charge of HIV-1 CRF01_AE V3 sequence regulates viral sensitivity to humoral immunity. *PLoS One* **3**, e3206 (2008).
19. Huang, C. C. *et al.* Structure of a V3-containing HIV-1 gp120 core. *Science* **310**, 1025–1028 (2005).
20. Clevestig, P., Pramanik, L., Leitner, T. & Ehrnst, A. CCR5 use by human immunodeficiency virus type 1 is associated closely with the gp120 V3 loop N-linked glycosylation site. *J. Gen. Virol.* **87**, 607–612 (2006).
21. Van Baelen, K. *et al.* HIV-1 coreceptor usage determination in clinical isolates using cloncal and population-based genotypic and phenotypic assays. *J. Virol. Methods* **146**, 61–73 (2007).
22. Schnur, E. *et al.* The conformation and orientation of a 27-residue CCR5 peptide in a ternary complex with HIV-1 gp120 and a CD4-mimic peptide. *J. Mol. Biol.* **410**, 778–797 (2011).
23. Pejchal, R. *et al.* A potent and broad neutralizing antibody recognizes and penetrates the HIV glycan shield. *Science* **334**, 1097–1103 (2011).
24. Kuwata, T. *et al.* Conformational epitope consisting of the V3 and V4 loops as a target for potent and broad neutralization of simian immunodeficiency viruses. *J. Virol.* **87**, 5424–5436 (2013).
25. Cecilia, D. *et al.* Neutralization profiles of primary human immunodeficiency virus type 1 isolates in the context of coreceptor usage. *J. Virol.* **72**, 6988–6996 (1998).
26. Brown, B. K. *et al.* Biologic and genetic characterization of a panel of 60 human immunodeficiency virus type 1 isolates, representing clades A, B, C, D, CRF01_AE, and CRF02_AG, for the development and assessment of candidate vaccines. *J. Virol.* **79**, 6089–6101 (2005).

27. Whitcomb, J. M. *et al.* Development and characterization of a novel single-cycle recombinant-virus assay to determine human immunodeficiency virus type 1 coreceptor tropism. *Antimicrob. Agents Chemother.* **51**, 566–575 (2007).
28. Jensen, M. A. & van't Wout, A. B. Predicting HIV-1 coreceptor usage with sequence analysis. *AIDS Rev.* **5**, 104–112 (2003).
29. Sing, T. *et al.* Predicting HIV coreceptor usage on the basis of genetic and clinical covariates. *Antivir. Ther.* **12**, 1097–1106 (2007).
30. Jensen, M. A. *et al.* Improved coreceptor usage prediction and genotypic monitoring of R5-to-X4 transition by motif analysis of human immunodeficiency virus type 1 env V3 loop sequences. *J. Virol.* **77**, 13376–13388 (2003).
31. Low, A. J. *et al.* Current V3 genotyping algorithms are inadequate for predicting X4 co-receptor usage in clinical isolates. *AIDS* **21**, F17–24 (2007).
32. Poveda, E. *et al.* Design and validation of new genotypic tools for easy and reliable estimation of HIV tropism before using CCR5 antagonists. *J. Antimicrob. Chemother.* **63**, 1006–1010 (2009).
33. Arroyo, M. A. *et al.* Virologic risk factors for vertical transmission of HIV type 1 in Puerto Rico. *AIDS Res. Hum. Retroviruses* **18**, 447–460 (2002).
34. Mörner, A. *et al.* Primary human immunodeficiency virus type 2 (HIV-2) isolates, like HIV-1 isolates, frequently use CCR5 but show promiscuity in coreceptor usage. *J. Virol.* **73**, 2343–2349 (1999).
35. Maeda, K. *et al.* Involvement of the second extracellular loop and transmembrane residues of CCR5 in inhibitor binding and HIV-1 fusion: insights into the mechanism of allosteric inhibition. *J. Mol. Biol.* **381**, 956–974 (2008).
36. Maeda, Y., Foda, M., Matsushita, S. & Harada, S. Involvement of both the V2 and V3 regions of the CCR5-tropic human immunodeficiency virus type 1 envelope in reduced sensitivity to macrophage inflammatory protein 1alpha. *J. Virol.* **74**, 1787–1793 (2000).
37. Koyanagi, Y. *et al.* Dual infection of the central nervous system by AIDS viruses with distinct cellular tropisms. *Science* **236**, 819–822 (1987).
38. Martí-Renom, M. A. *et al.* Comparative protein structure modeling of genes and genomes. *Annu. Rev. Biophys. Biomol. Struct.* **29**, 291–325 (2000).
39. Baker, D. & Sali, A. Protein structure prediction and structural genomics. *Science* **294**, 93–96 (2001).
40. Kollman, P. A. *et al.* Calculating structures and free energies of complex molecules: combining molecular mechanics and continuum models. *Acc. Chem. Res.* **33**, 889–897 (2000).
41. Pearlman, D. A. *et al.* AMBER, a package of computer programs for applying molecular mechanics, normal mode analysis, molecular dynamics and free energy calculations to simulate the structural and energetic properties of molecules. *Comp. Phys. Commun.* **91**, 1–41 (1995).
42. Hsieh, M. J. & Luo, R. Balancing Simulation Accuracy and Efficiency with the Amber United Atom Force Field. *J. Phys. Chem. B* **114**, 2886–2893 (2010).
43. Hawkins, G. D., Cramer, C. J. & Truhlar, D. G. Parametrized models of aqueous free energies of solvation based on pairwise descreening of solute atomic charges from a dielectric medium. *J. Phys. Chem.* **100**, 19824–19839 (1996).
44. Hawkins, G. D., Cramer, C. J. & Truhlar, D. G. Pairwise solute descreening of solute charges from a dielectric medium. *Chem. Phys. Lett.* **246**, 122–129 (1995).
45. Shao, J., Tanner, S. W., Thompson, N. & Cheatham, T. E. 3rd. Clustering molecular dynamics trajectories: 1. Characterizing the performance of different clustering algorithms. *J. Chem. Theory Comput.* **3**, 2312–2334 (2007).
46. Westervelt, P., Gendelman, H. E. & Ratner, L. Identification of a determinant within the human immunodeficiency virus 1 surface envelope glycoprotein critical for productive infection of primary monocytes. *Proc. Natl. Acad. Sci. U. S. A.* **88**, 3097–3101 (1991).
47. Jekle, A. *et al.* Coreceptor phenotype of natural human immunodeficiency virus with nef deleted evolves in vivo, leading to increased virulence. *J. Virol.* **76**, 6966–6973 (2002).

Acknowledgments

We thank Dr. Kenji Maeda, Experimental Retrovirology Section, HIV and AIDS Malignancy Branch, National Cancer Institute, National Institutes of Health, for providing plasmids and helpful suggestion, and Drs. Hiroaki Mitsuya and Hirotomo Nakata, Department of Infectious Diseases, Kumamoto University School of Medicine, for providing GHOST cell lines. We also thank the clinical and laboratory staffs of the AIDS Clinical Center, National Center for Global Health and Medicine, for their helpful support. This work was supported by a Grant-in-Aid for AIDS research from the Japanese Ministry of Health, Labour and Welfare (H23-AIDS-001), and the Global Center of Excellence Program (Global Education and Research Center Aiming at the Control of AIDS) from the Japanese Ministry of Education, Science, Sports, and Culture.

Author contributions

K.T. designed and performed the research, analyzed the data and wrote the manuscript. H.O. and H.S. performed MD simulation and calculation of the RMSD, wrote the manuscript. T.H. and J.K. performed the cloning and sequencing. S.O. designed and supervised the study. H.G. designed the study, analyzed the data, wrote and edited the manuscript. All authors read and approved the final manuscript.

Additional information

Supplementary information accompanies this paper at http://www.nature.com/scientificreports

Competing financial interests: S.O. has received honorariums and research grants from MSD, Janssen Pharmaceutical, Abbott, Roche Diagnostics, and Pfizer; has received honorariums from ViiV Healthcare, Torii Pharmaceutical, Bristol-Myers, Astellas Pharmaceutical, GlaxoSmithKline, Taisho Toyama Pharmaceutical, Dainippon Sumitomo Pharma, and Daiichisankyo. The remaining authors declare to have no conflict of interest.

How to cite this article: Tsuchiya, K. *et al.* Arginine insertion and loss of N-linked glycosylation site in HIV-1 envelope V3 region confer CXCR4-tropism. *Sci. Rep.* **3**, 2389; DOI:10.1038/srep02389 (2013).

Naturally Selected Rilpivirine-Resistant HIV-1 Variants by Host Cellular Immunity

Hiroyuki Gatanaga,[1,2] Hayato Murakoshi,[2] Atsuko Hachiya,[1,3] Tsunefusa Hayashida,[1,4] Takayuki Chikata,[2] Hirotaka Ode,[3,4] Kiyoto Tsuchiya,[1] Wataru Sugiura,[3] Masafumi Takiguchi,[2] and Shinichi Oka[1,2]

[1]AIDS Clinical Center, National Center for Global Health and Medicine, Tokyo; [2]Center for AIDS Research, Kumamoto University; [3]National Hospital Organization, Nagoya Medical Center; and [4]Japan Foundation for AIDS Prevention, Tokyo, Japan

Background. Rilpivirine is listed as an alternative key drug in current antiretroviral therapy (ART) guidelines. E138G/A/K in human immunodeficiency virus type 1 (HIV-1) reverse transcriptase (RT) are rilpivirine resistance-associated mutations and can be identified in a few ART-naive patients, although at low frequency. The 138th position in HIV-1 RT is located in one of the putative epitopes of human leukocyte antigen (HLA)–B*18–restricted cytotoxic T lymphocytes (CTLs). CTL-mediated immune pressure selects escape mutations within the CTL epitope. Here we tested whether E138G/A/K could be selected by HLA-B*18-restricted CTLs.

Methods. The amino acid variation at the 138th position was compared between ART-naive HIV-1–infected patients with and without HLA-B*18. The optimal epitope containing the 138th position was determined and the impact of E138G/A/K on CTL response was analyzed by epitope-specific CTLs. The effect of E138G/A/K on drug susceptibility was determined by constructing recombinant HIV-1 variants.

Results. The prevalence of E138G/A/K was 21% and 0.37% in 19 and 1088 patients with and without HLA-B*18, respectively (odds ratio, 72.3; $P = 4.9 \times 10^{-25}$). The CTL response was completely abolished by the substitution of E138G/A/K in the epitope peptide. E138G/A/K conferred 5.1-, 7.1-, and 2.7-fold resistance to rilpivirine, respectively.

Conclusions. E138G/A/K can be selected by HLA-B*18-restricted CTLs and confer significant rilpivirine resistance. We recommend drug resistance testing before the introduction of rilpivirine-based ART in HLA-B*18-positive patients.

Keywords. rilpivirine; E138G/A/K; HLA-B*18; CTL.

Rilpivirine is a new-generation nonnucleoside reverse transcriptase inhibitor (NNRTI), with noninferior clinical efficacy demonstrated in large clinical trials, compared with efavirenz [1, 2], and is listed as an alternative key drug in current antiretroviral therapy (ART) guidelines [3, 4]. In those clinical trials, rilpivirine showed more-favorable safety and tolerance profiles compared with efavirenz, although it was also associated with a higher virological failure rate. The most commonly observed NNRTI resistance-associated mutation in rilpivirine-treated patients with virological failure has so far been E138 K [1, 2]. Not only E138 K, but also other substitutions at the 138th position in human immunodeficiency virus type 1 (HIV-1) reverse transcriptase (RT), might confer significant rilpivirine resistance [5–7]. The glutamic acid at the 138th position (E138) is well conserved among HIV-1 strains and clinical isolates throughout clades [8]. However, some ART-naive patients are infected with HIV-1 variants harboring other amino acids at the 138th position (E138X), although the proportion of such patients is low [9]. The 138th position is located in one of the putative epitopes of human leukocyte antigen (HLA)–B*18-restricted cytotoxic T lymphocytes (CTLs) [10, 11]. Because CTL immune pressure often selects escape mutations within the epitope [11], E138X may be selected by HLA-B*18-restricted CTLs. In this study, we analyzed the frequency of amino acid variations at the 138th position in ART-naive patients with or without

Received 29 April 2013; accepted 13 June 2013; electronically published 23 June 2013.

Correspondence: Hiroyuki Gatanaga, MD, AIDS Clinical Center, National Center for Global Health and Medicine, 1-21-1 Toyama, Shinjuku-ku, Tokyo 162-8655, Japan (higatana@acc.ncgm.go.jp).

Clinical Infectious Diseases 2013;57(7):1051–5

DOI: 10.1093/cid/cit430

Table 1. Amino Acid Variations at the 138th Position of HIV-1 Reverse Transcriptase and Human Leukocyte Antigen–B*18

Amino Acid	HLA-B*18(+)	HLA-B*18(−)
E138 (wild-type)	15	1084
E138G	2	1
E138A	1	2
E138K	1	1

Abbreviation: HLA, human leukocyte antigen.

HLA-B*18, determined the impact of E138X on CTL response, and analyzed the drug susceptibility of recombinant HIV-1 variants harboring E138X.

METHODS

Sequences of HIV-1 Reverse Transcriptase

HIV-1 RT sequences were analyzed using viral RNA extracted from plasma samples [12], and HLA type was determined by standard sequence-based genotyping in 1107 ART-naive infected individuals who visited the Outpatient Clinic of the AIDS Clinical Center, National Center for Global Health and Medicine, Tokyo, between 2003 and 2012. The amino acid variation at the 138th position of HIV-1 RT was compared between individuals with and those without HLA-B*18, and the statistical significance of the difference was analyzed by Fisher exact test using the Statistical Package for Social Sciences, version 17.0 (SPSS, Chicago, Illinois). This study was approved by the institutional ethical committee of the National Center for Global Health and Medicine, and written informed consent was obtained from all the participants according to the Declaration of Helsinki.

Intracellular Cytokine Staining Assay

HIV-1-derived peptides and mutant peptides were synthesized using an automated multiple peptide synthesizer and purified by high-performance liquid chromatography. Peripheral blood mononuclear cells (PBMCs) from chronically HIV-1–infected HLA-B*18-positive patients were stimulated with the peptide (100 nM) in culture medium (RPMI 1640 medium supplemented with 10% fetal calf serum and 200 U/mL recombinant human interleukin 2). After 14 days in culture, the cells were assessed for interferon (IFN)–γ production activity using a FACSCanto II (BD Biosciences, San Jose, California) [13, 14].

Drug Susceptibility Assay

The desired mutations were introduced into the *XmaI-NheI* region of pTZNX, which encodes the 15th–267th positions of HIV-1 RT (strain BH10) [15, 16]. The *XmaI-NheI* fragment was inserted into pNL_{H219Q}, which was modified from pNL101 and encoded the full genome of HIV-1. Each molecular clone was transfected into COS-7 cells, and the obtained virions were harvested 48 hours after transfection and stored at −80°C until use. Efavirenz and nevirapine were generously provided by Merck Co, Inc (Rahway, New Jersey) and Boehringer Ingelheim Pharmaceutics Inc (Ridgefield, Connecticut), respectively. Etravirine and rilpivirine were purchased from Toronto Research Chemicals Inc (North York, Ontario, Canada). The susceptibility of recombinant HIV-1 variants to efavirenz, nevirapine, etravirine, and rilpivirine was determined in triplicate and repeated 3 times [16]. Fold resistance was calculated by comparing the viral 50% inhibitory concentration (IC_{50}) with that of monoclonal wild-type HIV-1.

Structural Modeling

We constructed structural models of the HIV-1 RT and rilpivirine complex by computational analysis, as described in our

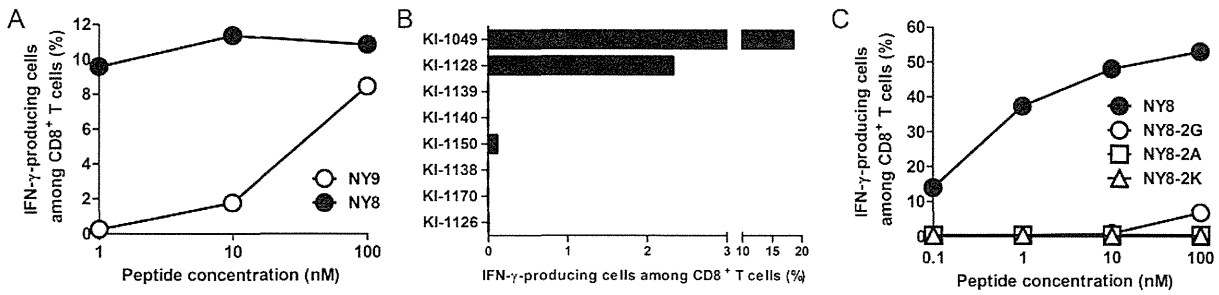

Figure 1. Recognition of human leukocyte antigen (HLA)–B*18-restricted $CD8^+$ T cells. *A*, Identification of the optimal epitope of HLA-B*18-restricted $CD8^+$ T cells. Peripheral blood mononuclear cells (PBMCs) from an HLA-B*18-positive individual chronically infected with human immunodeficiency virus type 1 (HIV-1) were stimulated with NY9 peptide and cultured for 2 weeks. Recognition of the bulk $CD8^+$ T cells toward each peptide was measured by the intracellular cytokine staining (ICS) assay. *B*, Induction of NY8-specific $CD8^+$ T cells in HLA-B*18-positive individuals chronically infected with HIV-1. PBMCs from 8 chronically HIV-1-infected HLA-B*18-positive individuals were stimulated with NY9 peptide and cultured for 2 weeks. Recognition of the bulk $CD8^+$ T cells toward NY8 peptide were measured by the ICS assay. *C*, Effects of E138G/A/K substitutions on the recognition of HLA-B*18-restricted $CD8^+$ T cells. Recognition of the bulk $CD8^+$ T cells toward each wild-type or mutant peptide was measured by the ICS assay. Abbreviations: IFN-γ, interferon gamma; NY8, NETPGIRY; NY8-2G, NGTPGIRY; NY8-2A, NATPGIRY; NY8-2 K, NKTPGIRY; NY9, NNETPGIRY.

Table 2. Susceptibility of Recombinant HIV-1 Variants to 4 Nonnucleoside Reverse Transcriptase Inhibitors

	IC_{50} (nM), Fold Resistance[a]			
Amino Acid	EFV	NVP	ETR	RPV
E138 (wild-type)	1.2 ± 0.2 (1)	31 ± 3 (1)	1.1 ± 0.1 (1)	0.16 ± 0.04 (1)
E138G	1.6 ± 0.2 (1.3)	30 ± 10 (0.97)	2.4 ± 0.3 (2.2)	0.82 ± 0.09 (5.1)
E138A	2.1 ± 0.3 (1.8)	30 ± 2 (0.97)	2.6 ± 0.2 (2.4)	1.13 ± 0.20 (7.1)
E138K	2.4 ± 0.4 (2.0)	50 ± 10 (1.6)	2.4 ± 0.1 (2.2)	0.43 ± 0.10 (2.7)

Data are presented as mean ± standard deviation.

Abbreviations: EFV, efavirenz; ETR, etravirine; IC_{50}, viral 50% inhibitory concentration; HIV-1, human immunodeficiency virus type 1; NVP, nevirapine; RPV, rilpivirine.

[a] Fold resistance was calculated by comparing viral IC_{50} with that of monoclonal wild-type HIV-1.

previous reports [15, 16]. In brief, the initial models of wild-type RT with rilpivirine were first constructed by homology modelling. The crystal structures of RT with NNRTI (PDB code: 2ZD1 [17]) was used for template structure. We also constructed the respective mutant RTs with rilpivirine by considering every possible conformer of the respective mutant models. The possible conformers were generated from the wild-type homology models using PyMOL software (http://www.pymol.org). Among the conformers, we selected those with the lowest energy as each mutant model.

RESULTS

First, we analyzed the frequency of amino acid variations at the 138th position of HIV-1 RT in 1107 ART-naive individuals. As expected, E138 was found in the majority (1099 cases [99%]) of the analyzed patients. However, 8 cases showed amino acid substitutions, including 3 cases of substitution with glycine (E138G), 3 cases with alanine (E138A), and 2 cases with lysine (E138 K). The frequency of E138G/A/K substitutions was 21% and 0.37% in 19 and 1088 individuals with and without HLA-B*18, respectively (Table 1). There was a significant difference in the frequency of the substitutions (odds ratio, 72.3; $P = 4.9 \times 10^{-25}$), suggesting that E138G/A/K could be selected by HLA-B*18-restricted CTLs.

Next, we delineated the impact of E138G/A/K on the response of HLA-B*18-restricted CTLs. The putative HLA-B*18-restricted CTL epitopes containing the 138th position of HIV-1 RT were NETPGIRYQY (NY10; position 137–146), NETPGIRYQ (NQ9; position 137–145), and NNETPGIRY (NY9; position 136–144) [10, 11]. These 3 peptides were used to stimulate PBMCs of 8 ART-treated HLA-B*18-positive patients chronically infected with HIV-1. IFN-γ production activity was detected in PBMCs from 1 of the 8 patients when stimulated with NY9. To determine the optimal epitope, the bulk $CD8^+$ T cells were further analyzed for NY9 and NETPGIRY (NY8; position 137–144). The bulk $CD8^+$ T cells more efficiently recognized NY8 than NY9 at 1-nM, 10-nM, and 100-nM concentrations (Figure 1*A*). These findings indicate that NY8 was the optimal epitope of HLA-B*18-restricted CTLs. Indeed, NY8-specific $CD8^+$ T cells were induced in 3 of the 8 patients (Figure 1*B*). A

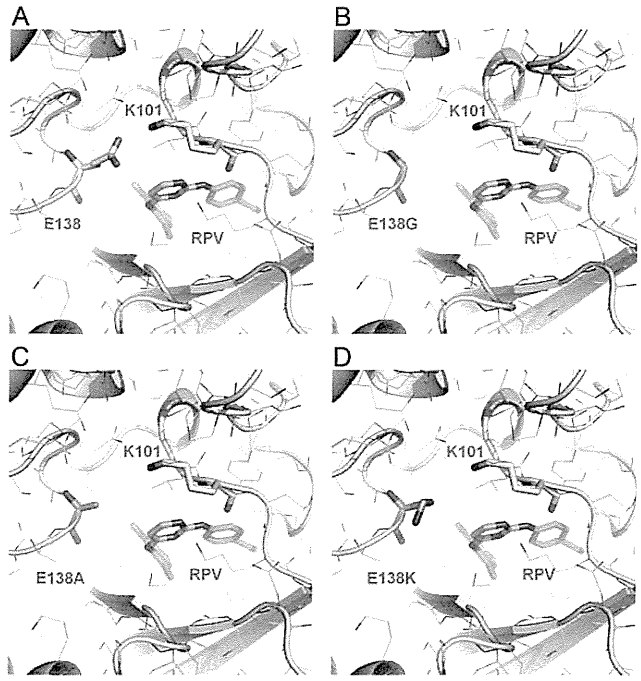

Figure 2. Structural models of human immunodeficiency virus type 1 reverse transcriptase (RT) and rilpivirine. The binding clefts of 4 complexes are shown: $RT_{E138(wild\text{-}type)}$ (*A*), RT_{E138G} (*B*), RT_{E138A} (*C*), and RT_{E138K} (*D*). Sticks indicate the amino acids at positions 101 and 138 of RT, and the atoms of rilpivirine. The mutated residues (E138G, E138A, and E138 K) and rilpivirine atoms are represented by orange and greenish-blue sticks, respectively. Abbreviation: RPV, rilpivirine.

previous study showed that HLA-B*18-binding peptides have 2 anchor residues, E at position 2 and Y/F at the C-terminus [18]. NY8 also had these 2 anchor residues, supporting that this peptide is a HLA-B*18-restricted CTL epitope. To analyze the effect of E138G/A/K on the CTL response, 3 mutant peptides, NGTPGIRY (NY8-2G), NATPGIRY (NY8-2A), and NKTPGIRY (NY8-2 K), were synthesized, and the recognition of the bulk CTLs for these mutant peptides was compared with that for NY8. The bulk CTLs failed to recognize these peptides at 0.1-nM, 1-nM, 10-nM, and 100-nM concentrations, although it effectively recognized NY8 (Figure 1*C*). These substitutions at the 138th position may affect peptide binding to the HLA-B*18 molecule because the second position of HLA-B*18-binding peptides is an anchor for HLA-B*18 [18]. These findings indicate that each of the E138G/A/K affected CTL recognition and allow escape from the HLA-B*18-restricted CTLs.

Finally, we analyzed the effect of E138G/A/K on viral susceptibility to NNRTIs by constructing recombinant HIV-1 variants. Each HIV-1 variant harboring one of E138G/A/K showed comparable replication fitness with wild-type HIV-1. Although the substitutions of E138G/A/K did not confer >2-fold resistance to efavirenz and nevirapine, they conferred mild resistance (2.2- to 2.4-fold) to etravirine. With regard to rilpivirine, E138 K, which was commonly observed in patients with virological failure under rilpivirine-based ART [1, 2], conferred mild resistance, whereas E138G and E138A conferred >5-fold resistance (Table 2). These findings indicate that in addition to E138 K, E138G and E138A can also reduce the clinical response to rilpivirine. The structural modeling suggests that substitution of E138 changes interactions around the rilpivirine-binding cleft (Figure 2). The side chain of E138 in the wild-type RT forms a salt bridge with the lysine at the 101th position (K101) at the edge of the cleft and establishes direct interactions with the pyrimidine moiety of rilpivirine, as seen in the crystal structure of RT with rilpivirine [17]. Meanwhile, mutant RTs with E138G/A/K substitutions could not create such a salt bridge, resulting in changes in the morphology of the binding cleft. In particular, RTs with E138G or E138A can reduce interactions with rilpivirine by creating large gaps between rilpivirine and the substituted 138th residues with small side chains, which seems to cause significant resistance to rilpivirine.

DISCUSSION

The major findings of the present study were as follows: (1) E138G/A/K substitutions were escape mutations of HLA-B*18-restricted CTLs and they were observed more frequently in HLA-B*18-positive patients than HLA-B*18-negative patients; and (2) we confirmed that these substitutions conferred significant resistance to rilpivirine, demonstrating that drug resistance–associated mutations can be selected naturally by CTL when its epitope is located in the viral protein of antiretroviral targets.

Studies of cellular immunology in HIV-1 have focused mainly on Gag [19, 20]. However, considering that many of the recently identified CTL epitopes are located in Pol [13, 14, 21], analysis of the interaction between CTL and drug susceptibility is warranted. Some escape mutations can persist after viral transmission to other hosts even if the new hosts do not have the corresponding HLAs [22]. Therefore, HIV-1 can adapt to HLA at a population level [23]. In fact, we identified E138G/A/K in ART-naive HLA-B*18-negative patients, although the frequency of such variations was extremely low. However, the same analysis performed in areas with higher prevalence of HLA-B*18, such as Eastern Europe [24], would probably detect higher frequency of E138G/A/K.

HIV drug resistance testing is recommended not only after treatment failure but also before the introduction of the initial treatment, considering the risk that the patient may have acquired drug-resistant viruses from those with treatment failure [3, 25]. The present study may add another reason for drug resistance testing of ART-naive patients: drug resistance–associated mutations may have evolved in the patients selected by their own immunity even if the original transmitted viruses were drug sensitive. At the very least, drug resistance testing should be performed before the introduction of rilpivirine-based ART in HLA-B*18-positive patients.

Notes

Acknowledgments. We thank all physicians and nurses at the AIDS Clinical Center, National Center for Global Health and Medicine, for the clinical practice and patient care. We also thank A. Nakano for the excellent project coordination.

Financial support. This work was supported in part by Grants-in Aid for AIDS research from the Ministry of Health, Labour, and Welfare, Japan; the Global COE Program (Global Education and Research center Aiming at the control of AIDS); MEXT, Japan; and Japan Foundation for AIDS Prevention.

Potential conflicts of interest. H. G. has received honoraria from ViiV Healthcare, MSD K.K., Abbott Japan, Janssen Pharmaceutical K.K., and Torii Pharmaceutical. S. O. has received honoraria and research grants from MSD K.K., Abbott Japan, Janssen Pharmaceutical K.K., Pfizer, ViiV Healthcare, and Roche Diagnostics K.K., and has received honoraria from Astellas Pharmaceutical K.K., Bristol-Myers K.K., Daiichisankyo, Dainippon Sumitomo Pharma, GlaxoSmithKline, K.K., Taisho Toyama Pharmaceutical, and Torii Pharmaceutical. All other authors report no potential conflicts.

All authors have submitted the ICMJE Form for Disclosure of Potential Conflicts of Interest. Conflicts that the editors consider relevant to the content of the manuscript have been disclosed.

References

1. Molina JM, Cahn P, Grinsztejn B, et al. Rilpivirine versus efavirenz with tenofovir and emtricitabine in treatment-naïve adults infected with HIV-1 (ECHO): a phase 3 randomised double-blind active-controlled trial. Lancet **2011**; 378:238–46.
2. Cohen CJ, Andrade-Vilanueva J, Clotet B, et al. Rilpivirine versus efavirenz with two background nucleoside or nucleotide reverse

transcriptase inhibitors in treatment-naïve adults infected with HIV-1 (THRIVE): a phase 3, randomised, non-inferiority trial. Lancet **2011**; 378:229–37.
3. Department of Health and Human Services Panel on Antiretroviral Guidelines for Adult and Adolescents. Guidelines for the use of antiretroviral agents in HIV-1-infected adults and adolescents. http://www.aidsinfo.nih.gov/ContentFiles/AdultandAdolescentGL.pdf. Accessed 26 March 2013.
4. Thompson MA, Aberg JA, Hoy JF, et al. Antiretroviral treatment of adult HIV infection: 2012 recommendations of the International Antiviral Society–USA panel. JAMA **2012**; 308:387–402.
5. Johnson VA, Calvez V, Gunthard HF, et al. Update of the drug resistance mutations in HIV-1: March 2013. Top Antivir Med **2013**; 21:6–14.
6. Azunj H, Tirry I, Vingerhoets J, et al. TMC278, a next-generation nonnucleoside reverse transcriptase inhibitor (NNRTI), active against wild-type and NNRTI-resistant HIV-1. Antimicrob Agents Chemother **2010**; 54:718–27.
7. Asahchop EL, Wainberg MA, Oliveira M, et al. Distinct resistance patterns to etravirine and rilpivirine in viruses containing nonnucleoside reverse transcriptase inhibitor mutations at baseline. AIDS **2013**; 27:879–87.
8. Lambert-Niclot S, Charpentier C, Storto A, et al. Prevalence of preexisting resistance-associated mutations to rilpivirine, emtricitabine and tenofovir in antiretroviral-naive patients infected with B and non-B subtype HIV-1 viruses. J Antimicrob Chemother **2013**; 68:1237–42.
9. Siegel MO, Swierzbinski M, Kan VL, Parenti DM. Baseline E138 reverse transcriptase resistance-associated mutations in antiretroviral-naive HIV-infected patients. AIDS **2012**; 26:1181–2.
10. Liu Y, McNevin J, Cao J, et al. Selection on the human immunodeficiency virus type 1 proteome following primary infection. J Virol **2006**; 80:9519–29.
11. Brumme ZL, John M, Carlson JM, et al. HLA-associated immune escape pathways in HIV-1 subtype B Gag, Pol and Nef proteins. PLoS One **2009**; 4:e6687.
12. Gatanaga H, Ibe S, Matsuda M, et al. Drug-resistant HIV-1 prevalence in patients newly diagnosed with HIV/AIDS in Japan. Antiviral Res **2007**; 75:75–82.
13. Honda K, Zheng N, Murakoshi H, et al. Selection of escape mutant by HLA-C-restricted HIV-1 Pol-specific T lymphocytes carrying strong ability to suppress HIV-1 replication. Eur J Immunol **2011**; 41:97–106.
14. Watanabe T, Murakoshi H, Gatanaga H, et al. Effective recognition of HIV-1-infected cells by HIV-1 integrase-specific HLA-B*4002-restricted T cells. Microbes Infect **2011**; 13:160–6.
15. Gatanaga H, Ode H, Hachiya A, Hayashida T, Sato H, Oka S. Impact of human leukocyte antigen-B*51-restricted cytotoxic T-lymphocyte pressure on mutation patterns of nonnucleoside reverse transcriptase inhibitor resistance. AIDS **2010**; 24:F15–22.
16. Gatanaga H, Ode H, Hachiya A, Hayashida T, Sato H, Oka S. Combination of V106I and V179D polymorphic mutations in human immunodeficiency virus type 1 reverse transcriptase confers resistance to efavirenz and nevirapine but not etravirine. Antimicrob Agents Chemother **2010**; 54:1596–602.
17. Das K, Bauman JD, Clark AD Jr, et al. High-resolution structures of HIV-1 reverse transcriptase/TMC278 complexes: strategic flexibility explains potency against resistance mutations. Proc Natl Acad Sci U S A **2008**; 105:1466–71.
18. Hickman HD, Luis AD, Buchli R, et al. Toward a definition of self: proteomic evaluation of the class I peptide repertoire. J Immunol **2004**; 172:2944–52.
19. Brumme ZL, Tao I, Szeto S, et al. Human leukocyte antigen-specific polymorphisms in HIV-1 Gag and their association with viral load in chronic untreated infection. AIDS **2008**; 22:1277–86.
20. Martinez-Picado J, Prado JG, Fry EE, et al. Fitness const of escape mutations in p24 Gag in association with control of human immunodeficiency virus type 1. J Virol **2006**; 80:3617–23.
21. Brumme ZL, Brumme CJ, Carlson J, et al. Marked epitope- and allele-specific differences in rates of mutation in human immunodeficiency virus type 1 (HIV-1) Gag, Pol, and Nef cytotoxic T-lymphocyte epitopes in acute/early HIV-1 infection. J Virol **2008**; 82:9216–27.
22. Goulder PJ, Brander C, Tang Y, et al. Evolution and transmission of stable CTL escape mutations in HIV infection. Nature **2001**; 412:334–8.
23. Kawashima Y, Pfafferott K, Frater J, et al. Adaptation of HIV-1 to human leukocyte antigen class I. Nature **2009**; 458:641–5.
24. Solberg OD, Mack SJ, Lancaster AK, et al. Balancing selection and heterogeneity across the classic human leukocyte antigen loci: a meta-analytic review of 497 population studies. Hum Immunol **2008**; 69: 443–64.
25. Hirsh MS, Gunthard HF, Schapiro JM, et al. Antiretroviral drug resistance testing in adult HIV-1 infection. Clin Infect Dis **2008**; 47: 266–85.

PLOS ONE

Is Ritonavir-Boosted Atazanavir a Risk for Cholelithiasis Compared to Other Protease Inhibitors?

Yohei Hamada[1], Takeshi Nishijima[1,3], Hirokazu Komatsu[2], Katsuji Teruya[1], Hiroyuki Gatanaga[1,3]*, Yoshimi Kikuchi[1], Shinichi Oka[1,3]

1 AIDS Clinical Center, National Center for Global Health and Medicine, Tokyo, Japan, **2** Department of Community Care, Saku Central Hospital, Nagano, Japan, **3** Center for AIDS Research, Kumamoto University, Kumamoto, Japan

Abstract

Objective: To compare the incidence of complicated cholelithiasis in patients receiving ritonavir-boosted atazanavir (ATV/r)-containing antiretroviral therapy with those on other protease inhibitors (PIs).

Design: We conducted a single-center retrospective cohort study of patients who started either ritonavir-boosted ATV/r- or other PIs (ritonavir-boosted fosamprenavir, unboosted fosamprenavir, lopinavir/ritonavir, and ritonavir-boosted darunavir) -containing antiretroviral therapy.

Methods: The incidence of complicated cholelithiasis was determined in each group. Complicated cholelithiasis was defined as follows: 1) cholelithiasis complicated by cholecystitis, cholangitis, or pancreatitis or 2) symptomatic cholelithiasis or choledocholithiasis which required invasive procedures such as cholecystomy and endoscopic retrograde cholangiopancreatography. The effects of ATV/r were estimated by univariate and multivariate Cox hazards models as the primary exposure.

Results: Complicated cholelithiasis was diagnosed in 3 patients (2.23 per 1000 person-years) in the ATV/r group (n = 466), and 3 (1.64 per 1000 person-years) in the other PIs group (n = 776), respectively. The incidence was not statistically different in the two groups by log-rank test (P = 0.702). By univariate and multivariate analysis adjusted for age and body weight, ATV/r use was not associated with cholelithiasis. (HR = 1.365; 95% CI, 0.275–6.775; p = 0.704) (adjusted HR = 1.390; 95% CI, 0.276–7.017; p = 0.690). For the 3 patients who developed cholelithiasis in the ATV/r group, the time to the diagnosis of cholelithiasis was 18, 34, and 39 months, respectively.

Conclusion: In this study, the incidence of complicated cholelithiasis was low and was not different between patients on ATV/r and those on other PIs. On the contrary to ATV/r-associated nephrolithiasis, the possible risk of cholelithiasis should not preclude the use of ATV/r.

Citation: Hamada Y, Nishijima T, Komatsu H, Teruya K, Gatanaga H, et al. (2013) Is Ritonavir-Boosted Atazanavir a Risk for Cholelithiasis Compared to Other Protease Inhibitors? PLoS ONE 8(7): e69845. doi:10.1371/journal.pone.0069845

Editor: Wenzhe Ho, Temple University School of Medicine, United States of America

Received February 2, 2013; **Accepted** June 12, 2013; **Published** July 16, 2013

Funding: This work was supported by a Grant-in-Aid for AIDS research from the Ministry of Health, Labor, and Welfare, Japan (H23-AIDS-001), and the Global Center of Excellence Program from the Ministry of Education, Science, Sports and Culture of Japan. The funders had no role in study design, data collection and analysis, decision to publish, or preparation of the manuscript.

Competing Interests: S.O. has received honorarium and a research grant from MSD K.K., Abbott Japan, Co., Janssen Pharmaceutical K.K., Pfizer, Co., and Roche Diagnostics K.K.; has received honorarium from Astellas Pharmaceutical K.K., Bristol-Myers K.K., Daiichisankyo, Co., Dainippon Sumitomo Pharma, Co., GlaxoSmithKline, K.K., Taisho Toyama Pharmaceutical, Co., Torii Pharmaceutical, Co., and ViiV Healthcare. H.G. has received honorarium from MSD K.K., Abbott Japan, Co., Janssen Pharmaceutical K.K., Torii Pharmaceutical, Co., and ViiV Healthcare, Co. The other authors declare no conflicts of interest, and this does not alter the authors' adherence to all the PLOS ONE policies on sharing data and materials.

* E-mail: higatana@acc.ncgm.go.jp

Introduction

Ritonavir-boosted atazanavir (ATV/r) is a widely used protease inhibitor (PI) in combination with other antiretroviral drugs for patients with human immunodeficiency virus-1 (HIV) infection (URL: http://aidsinfo.nih.gov/contentfiles/lvguidelines/adultandadolescentgl.pdf) (URL: http://www.europeanaidsclinicalsociety.org/images/stories/EACS-Pdf/EacsGuidelines-v6.1-2edition.pdf). ATV/r is one of the first-line antiretroviral drugs based on its high efficacy, tolerability, favorable lipid profile, and once-daily dosing [1,2]. However, recent studies suggested potential adverse effects associated with ATV/r, including nephrolithiasis and cholelithiasis [3,4].

Previous studies suggested a possible causal relation between protease inhibitors and cholelithiasis [4–8]. Of the 20 previously reported patients with PI-associated cholelithiasis, 16 (80%) were associated with the use of ATV [4–8]. In one of these studies, which reported 14 patients with ATV-associated cholelithiasis, the median duration of atazanavir exposure was 42 months, suggesting that prolonged exposure to ATV is a possible risk for cholelithiasis [4]. However, there is virtually no information on the incidence of ATV/r-related cholelithiasis compared to other PIs although ATV/r is one of the most frequently prescribed PIs.

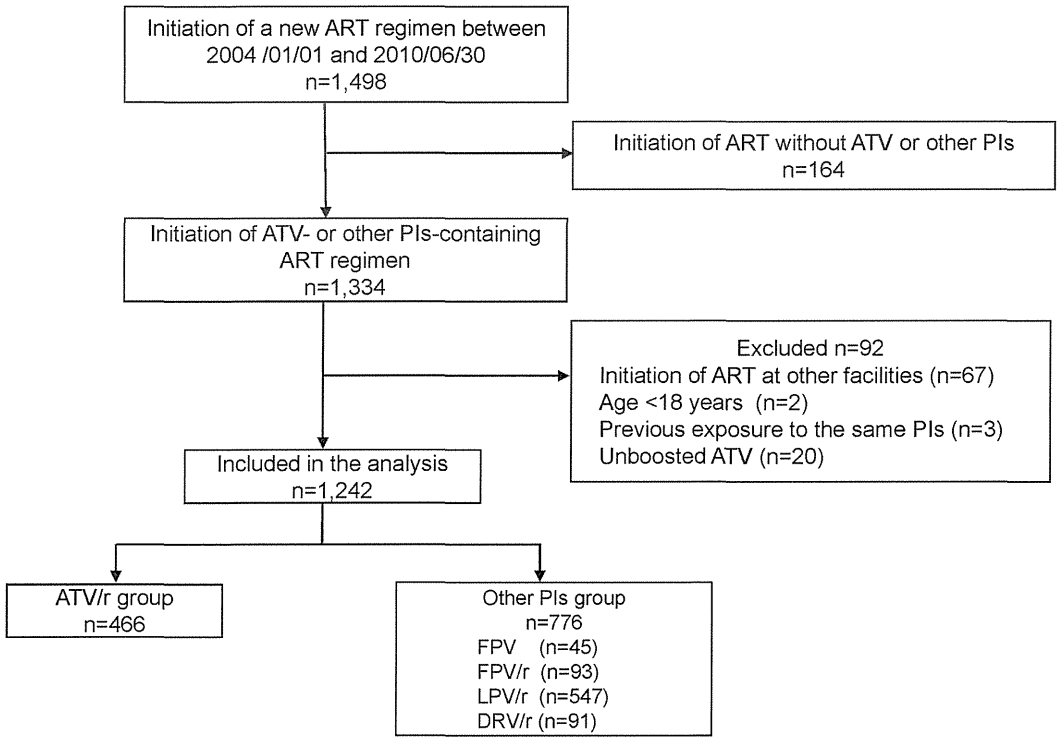

Figure 1. Flow diagram of patient selection. ART, antiretroviral treatment; ATV, atazanavir; PIs, protease inhibitors; LPV/r, lopinavir/ritonavir; ATV/r, ritonavir-boosted atazanavir; FPV, fosamprenavir; FPV/r, ritonavir-boosted fosamprenavir; DRV/r, ritonavir-boosted darunavir.
doi:10.1371/journal.pone.0069845.g001

Thus, we conducted a retrospective study to compare the incidence of complicated cholelithiasis in patients on ATV/r-containing antiretroviral treatment (ART) and those on other commonly used PIs [unboosted fosamprenavir (FPV), ritonavir-boosted fosamprenavir (FPV/r), lopinavir/ritonavir (LPV/r), and ritonavir-boosted darunavir (DRV/r)].

Table 1. Baseline demographics and laboratory data of patients who received ATV/r- and other-PIs-containing antiretroviral therapy (n = 1,242).

	ATV/r (n = 466)	Other PIs (n = 776)	P value
Age* [SD]	39.0 [10.6]	40.0 [11.5]	0.132
Male gender (%)	434 (93.1)	714 (91.9)	0.422
Race (East Asian origin) (%)	449 (96.4)	722 (93.0)	0.015
Body weight (kg)* [SD]	65.0 [10.5]	62.1 [10.7]	<0.001
BMI (kg/m^2)* [SD]	22.7 [3.14]	21.7 [3.25]	<0.001
CD4 count (/μl)* [SD]	304.0 [184.5]	176.2 [170.8]	<0.001
HIV viral load (log_{10}/ml)* [SD]	3.58 [1.38]	4.42 [1.40]	<0.001
Treatment naïve (%)	282 (60.5)	556 (71.6)	<0.001
TDF use (%)	177 (38.0)	326 (42.0)	0.162
eGFR (ml/min/1.73 m^2)* [SD]	117.4 [38.1]	121.7 [33.7]	0.012
Hepatitis B or C (%)	57 (12.2)	111 (14.3)	0.301

*Arithmetic mean.
ATV/r: ritonavir-boosted atazanavir, PI: protease inhibitor, SD: standard deviation, BMI: body mass index, TDF: tenofovir, eGFR: estimated glomerular filtration rate.
doi:10.1371/journal.pone.0069845.t001

Methods

Ethics statement

This study was approved by the Human Research Ethics Committee of National Center for Global Health and Medicine, Tokyo. All patients included in this study provided a written informed consent for their clinical and laboratory data to be used and published for research purposes. This study has been conducted according to the principles expressed in the Declaration of Helsinki (http://www.wma.net/en/30publications/10policies/b3/17c.pdf).

Study Subjects

This is a retrospective, single-center cohort study of patients with HIV-1 infection using the medical records at the National Center for Global Health and Medicine, Tokyo, Japan. Our facility is one of the largest clinics for patients with HIV infection in Japan with more than 2,700 registered patients. The study population was HIV infected patients, aged >17 years, who commenced treatment with ATV/r, FPV/r, FPV, LPV/r, or DRV/r-containing ART between January 1, 2004 and June 30, 2010. Both treatment-naïve and treatment-experienced patients were included. The follow-up period started at the time of commencement of ART for the first time during the study period, and ended June 30, 2011. Patients were excluded; 1) if they had started the abovementioned ART during the study period at other facilities, 2) if they were prescribed unboosted ATV. Patients with previous exposure to one of the abovementioned drugs before the present study and commenced the same drug in this study were also excluded from the analysis.

The attending physician selected the PI drug at baseline, based on the Japanese guidelines, which placed all of the above-

Table 2. Uni-and multi-variate analyses to estimate the risk of ATV/r use over other PIs-containing antiretroviral therapies for cholelithiasis.

	Model 1 crude (n = 1,242)			Model 2 adjusted (n = 1,203)		
	HR	95%CI	P value	HR	95%CI	P value
ATV/r use	1.365	0.275–6.775	0.702	1.390	0.276–7.017	0.689
Age per 1 year	1.072	1.021–1.127	0.006			
Male gender	0.446	0.052–3.831	0.463			
Race (East Asian origin)	0.285	0.033–2.444	0.252			
Weight per 1 kg increment	0.990	0.914–1.073	0.807			
BMI per 1 kg/m^2 increment	0.997	0.780–1.274	0.980			
CD4 count per 10/μl increment	0.987	0.938–1.038	0.605			
HIV viral load per log10/ml increment	0.917	0.541–1.557	0.750			
Baseline eGFR 10 ml/min/1.73 m^2 decrement	1.140	0.842–1.557	0.394			
Hepatitis B or Hepatitis C	0.040	0.000–1138.5	0.538			

Model 2 was adjusted for age and body weight.
HR: hazard ratio, CI: confidential interval, ATV/r: ritonavir-boosted atazanavir, BMI: body mass index, eGFR: estimated glomerular filtration rate.
doi:10.1371/journal.pone.0069845.t002

mentioned drugs as the preferred choice, at least for 3 years during the study period (http://www.haart-support.jp/guideline2011.

pdf. in Japanese). The attending physician also selected the concurrent drugs, including nucleoside reverse transcriptase inhibitors (NRTI), non-NRTI, integrase inhibitors, and CCR5 inhibitors. None of the patients received two PIs during the study period.

Measurements

Complicated cholelithiasis was defined as follows: 1) cholelithiasis diagnosed by computed tomography or abdominal ultrasonography, together with cholecystitis, cholangitis, or pancreatitis, or 2) symptomatic cholelithiasis or choledocholithiasis requiring invasive procedures, such as cholecystomy or endoscopic retrograde cholangiopancreatography. Before the initiation of ART and until suppression of HIV-1 viral load, patients visited our clinic every month. However, after viral load suppression, the visit interval was extended up to every three months.

In this study, the primary exposure variable was ATV/r use over other PIs (FPV, FPV/r, LPV/r, and DRV/r). The potential risk factors for cholelithiasis were determined according to previous studies and collected from the medical records, together with the basic demographics [4,9,10]. They included age, sex, body weight, body mass index (BMI), baseline laboratory data [CD4 cell count, HIV viral load, estimated glomerular filtration rate (eGFR)], and presence or absence of other medical conditions [concurrent use of tenofovir (TDF), co-infection with hepatitis B, defined by positive hepatitis B surface antigen, and co-infection with hepatitis C, defined by positive hepatitis C viral load]. eGFR was calculated as described previously [11]. At our clinic, weight was measured on every visit whereas other variables were measured in the first visit and at least once annually. We used the data on or closest to and preceding the day of starting ART by no more than 180 days.

Statistical analysis

Baseline characteristics were compared using the unpaired Student's *t*-test or χ^2test (Fisher's exact test) for quantitative or qualitative variables, respectively. The time to the diagnosis of complicated cholelithiasis was calculated from the date of commencement of pre-defined PI-containing ART to the date of diagnosis of cholelithiasis. Censored cases represented those who discontinued the PIs, dropped out, were referred to other facilities, or at the end of follow-up period. The time from the start of ART to the diagnosis of cholelithiasis was analyzed by the Kaplan Meier method for patients who started ATV/r (ATV/r group) or other PIs (other PIs group), and the log-rank test was used to determine the statistical significance. The Cox proportional hazards regression analysis was used to estimate the impact of ATV/r use over other PIs on the incidence of cholelithiasis. The impact of each parameter listed above was also estimated by univariate Cox proportional hazards regression. We conducted multivariate analysis adjusted for age and body weight only, because of the small number of cases that were diagnosed with complicated cholelithiasis.

Statistical significance was defined as two-sided p value <0.05. We used the hazard ratio (HR) and 95% confidence interval (95%CI) to estimate the impact of each variable on cholelithiasis. All statistical analyses were performed with The Statistical Package for Social Sciences ver. 17.0 (SPSS, Chicago, IL).

Results

A total of 1,498 patients commenced or switched key drugs (PIs, non-NRTIs, or integrase inhibitor) between January 1, 2004 and June 30, 2010. Of the 1,242 patients who were included in the analysis, 466 (37.5%) started ATV/r-containing ART while 776 (62.5%) started other PIs-containing ART (Figure 1). Table 1 shows the demographics, laboratory data, and medical conditions of the study population at baseline. The majority of the study population was males, of East Asian origin, and comparatively young. The ATV/r group included significantly more patients of East Asian origin ($p = 0.015$) with significantly higher body weight ($P<0.001$), higher CD4 count ($p<0.001$), lower viral load ($p<0.001$), and lower eGFR ($P = 0.012$), compared with other PI groups. In contrast, patients of the other PIs group were significantly more likely to be treatment naïve ($p<0.001$). However, all other major background parameters were similar in the two groups.

Cholelithiasis was diagnosed in 3 patients (0.64%) of the ATV/r group and 3 (0.39%) in the other PIs group, with an estimated